The mechanical properties and hydrogen embrittlement of ~~hydrogen~~ scandium

Michael Paul Zalesky

Under the supervision of Dr. T. E. Scott

From the Department of Metallurgy

Iowa State University

Abstract

The strength and ductility of polycrystalline scandium have been studied as a function of hydrogen concentration and test temperature. The effects of hydrogen on the mechanical behavior of scandium are discussed in terms of current embrittlement concepts for hydride forming metals. Hydrogen concentrations ranging from 0.20 to 20.83 atomic percent and temperatures from 78 to 473K were employed in this investigation. SEM fractographs are shown to illustrate the modes of tensile failure.

---

[1]DOE REPORT IS-T-918. This work was performed under Contract W-7405-eng-82 with the Department of Energy.

The mechanical properties and hydrogen embrittlement of scandium

by

Michael Paul Zalesky

A Thesis Submitted to the
Graduate Faculty in Partial Fulfillment of
The Requirements for the Degree of
MASTER OF SCIENCE

Department: Materials Science and Engineering
Major: Metallurgy

Signatures have been redacted for privacy

Iowa State University
Ames, Iowa

1980

TABLE OF CONTENTS

DEDICATION

I would like to dedicate this work to my mother, and to my father who never saw his son grow up.

PART I. MECHANICAL PROPERTIES OF SCANDIUM

INTRODUCTION

The hexagonal close packed (HCP) metal scandium is chemically similar to and is generally included with the rare earth metals. It is the first transition metal in the periodic table. Even though scandium is the thirty-sixth most abundant element (1), it has not found industrial application as have lead, molybdenum and antimony which are less abundant. The reason for this dearth of commercial markets is that scandium is dispersed in quantities less than 100 parts per million throughout the earth's crust. Most of the scandium consumed in the world is derived from uranium tailings where the concentrations are quite small, less than 1000 parts per million (1, p. 66). Because it is difficult to concentrate scandium ore and then to extract and purify the metal, scandium has been used primarily in research.

Mechanical property data on relatively pure scandium has been confined primarily to hardness measurements (2,3). Geiselman (4) and Sokolov et al. (5) have measured its yield strength, ultimate strength and ductility as functions of strain rate and temperature. Discrepancies in the mechanical property data reported by Geiselman and Sokolov are evident and, probably, attributable to impurity effects. The scandium available at the Ames Laboratory is purer, and since tensile samples were being prepared for other purposes, it seemed appropriate to investigate the mechanical properties of the "pure" scandium metal.

MATERIALS AND SAMPLE PREPARATION

Scandium used in this investigation was prepared at the Ames Laboratory by the calcium reduction of scandium fluoride in a tantalum crucible (6). The as-cast material was arc-melted, under purified argon, into finger-shaped ingots which were encapsulated in stainless steel tubing while under an argon atmosphere. The jacketed fingers were reduced to rods having a diameter of 0.64 cm by swaging at 853 K. After the jackets were removed mechanically, the rods were further reduced to a diameter of 0.51 cm by swaging at room temperature. The cold-worked rods were chemically cleaned, electropolished in a 6% perchloric acid 94% methanol electrolyte maintained at 200 K, and annealed for 1 hr at 1023 K under a vacuum of 1.35×10^{-5} Pa. The rods were then reduced to a final diameter of 0.26 cm by a series of room temperature swaging reductions of approximately 30% each followed by intermediate cleaning, electropolishing and vacuum annealing for 45 min at 1023 K. Subsequently, the rods were cut to 5 cm length and a 2.54 cm gage length of diameter 0.2 cm was machined in each by centerless grinding. Tool marks were removed from the machined tensile specimens by a final electropolish. Annealing of the specimens was carried-out in vacuum for 120 min at 1023 K. A number of specimens annealed at 1023 K were wrapped in zirconium sheet and sealed in a quartz tube under vacuum for further heat-treatment designed to increase the grain size. Thermal treatment consisted of placing the quartz tubes in a furnace maintained at 1130 K for 135 min before furnace cooling. Grain size determinations were

performed on several samples using the intercept method described by Hilliard (7). The results showed uniform equiaxed grains with an average diameter of 80 μm for the first heat-treatment, while the second heat-treatment produced grains of varying size, with an average diameter of 140 μm. Chemical analyses of the scandium used in this investigation and the scandium used by Geiselman (4) and Sokolov et al. (5) are given in Table 1.

Table 1. Chemical composition of scandium[a], ppm by weight

	H	O	N	C	Al	Si	Fe	Cu	R.E.[b]	Others[c]
Ames Lab Scandium	15 (48 ± 8)[d]	152 (140 ± 52)[d]	16 (7 ± 4)[d]	99	<10	<10	<40	<20	<60	<5
Sokolov[e]										
Geiselman[f]	200	4000	100							

[a]Analysis of as-received metal. H, N, and O by vacuum fusion; C by combustion; others spectrographic methods.

[b]All rare-earth elements combined.

[c]Other elements less than 5 ppm by weight each.

[d]Analyzed after testing. Average values of 20 samples.

[e]Claimed 99.99 percent purity, but no analysis given.

[f]Only interstitials are reported.

EXPERIMENTAL PROCEDURE

Tensile tests were done on a 44.5 KN capacity Instron TT-C tensile machine. A stainless steel cage assembly attached beneath the lower cross-head of the tensile machine allowed test temperatures to be attained by immersing the assembly in suitable constant temperature baths. Subambient test temperatures were achieved by using a liquid isopentane bath cooled by a liquid nitrogen heat exchanger. In order to avoid temperature gradients within the bath, nitrogen was allowed to bubble continuously. A stirred silicon oil bath heated by an immersion heating coil was used for temperatures of 373 K and 473 K. Temperatures were maintained to ±2 K, as recorded by a thermocouple attached to the testing cage at a position 1 cm from the center of the specimen.

True stress-true strain curves and strain rate sensitivity data were obtained from load-elongation curves. The yield strength in all cases was obtained from the 0.2% offset stress after correcting for machine deflection. The strain rate employed during tensile testing was 3.33×10^{-5} sec^{-1}. Duplicate tests were made on the 80 μm grain size tensile specimens whereas only single tests were made on the 140 μm grain size material. The strain rate sensitivity measurements were made by changing the cross-head speed cyclically between values corresponding to 3.33×10^{-5} sec^{-1} and 3.33×10^{-3} sec^{-1}.

True stress and true strain were calculated from the load-elongation curves using the following relations,

$$e = (\ell - \ell_0)/\ell_0 \tag{1}$$

where e = engineering strain

ℓ = final gage length

ℓ_0 = initial gage length

$$\sigma = P/A(e+1) \tag{2}$$

where σ = true stress

P = applied load as read from a load-elongation curve

A = initial cross-sectional area

e = engineering strain

$$\varepsilon = \ln(e+1) \tag{3}$$

where ε = true strain

e = engineering strain.

The strain rate sensitivity parameter 'm' was calculated from measured changes in flow stress, brought about by changes in strain rate at constant temperature and strain using the equation

$$m = \log(P_2/P_1)/\log(\dot{\varepsilon}_2/\dot{\varepsilon}_1) \tag{4}$$

where P = applied load

$\dot{\varepsilon}$ = strain rate

In the above expression only changes in load were taken into account instead of stress, because the cross-sectional area does not change during an instantaneous strain rate change at constant strain.

For a single thermally activated mechanism, the activation volume V is given by

$$V = kT(\partial \ln \dot{\varepsilon}/\partial \tau)_T \qquad (5)$$

where k = Boltzman constant

T = absolute temperature

$\dot{\varepsilon}$ = strain rate

τ = shear stress.

However in order to apply the above relationship to polycrystalline data, true stress has to be related to shear stress by the relationship

$$\tau = \sigma/M \qquad (6)$$

where τ = shear stress

σ = true stress

M = average Taylor factor.

Since there is no general agreement on the correct Taylor factor for hexagonal close packed structures, the activation volume referred to

in this investigation will be a pseudo activation volume V^* given by

$$V^* = kT(\partial \ln \dot{\varepsilon}/\partial \sigma)_T = kT[(\ln \dot{\varepsilon}_2/\dot{\varepsilon}_1)/(\sigma_2-\sigma_1)]_T = V/M. \qquad (7)$$

EXPERIMENTAL RESULTS

Stress-Strain Characteristics

True stress-true strain curves for 80 μm and 140 μm grain size scandium specimens are shown in Figs. 1 and 2, respectively. There was no indication of a discontinuous yield point or serrated stress-strain behavior and none of the specimens necked significantly or exhibited macroscopic flow localization at any temperature in the range of temperatures examined. The curves shown in Figs. 1 and 2 are only plotted to maximum load; however, beyond maximum load only a small amount of unloading occurred before fracture. A representative load-elongation curve illustrating this point is shown in Fig. 3.

Comparison of curves for the same test temperature in Figs. 1 and 2 reveals that grain size had little effect on the stress-strain behavior of scandium. More precisely, however, there was no grain size effect at 78 K or 373 K while the 140 μm material exhibited higher stress values at all strains at 200 K and lower stress values at all strains at 295 K.

Log true stress versus log true strain plots for 80 μm and 140 μm grain size scandium specimens are presented in Figs. 4 and 5, respectively. In these figures total strain is indicated because it was impossible to determine the elastic region accurately. Two distinctly different regions of behavior are noticeable with the transition occurring at a strain of about 0.01 at all temperatures except 78 K, where the change occurs at 0.03 strain. In the upper strain region shown in Figs. 4 and 5,

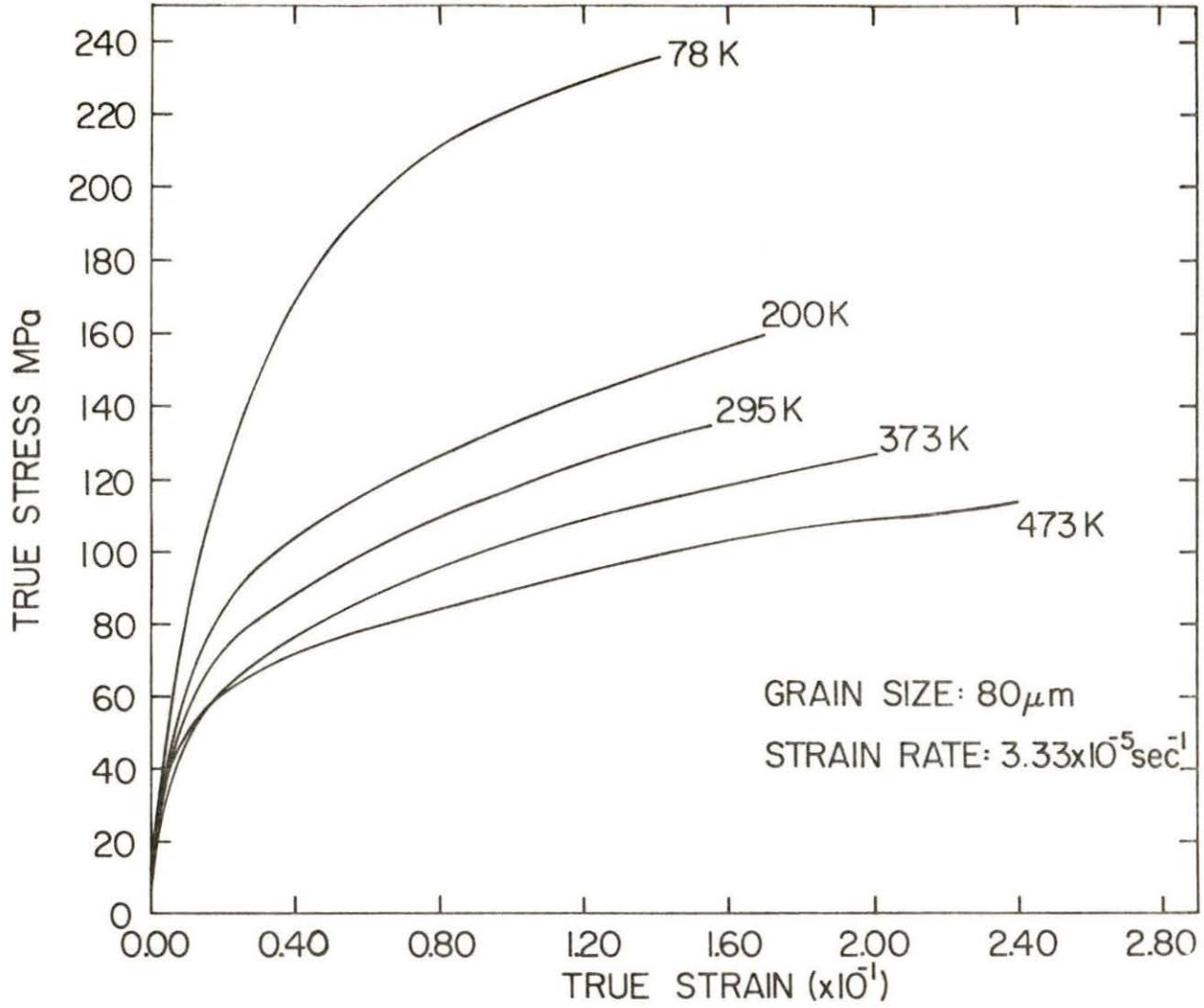

Fig. 1. True stress versus true strain for 80 μm grain size at various temperatures

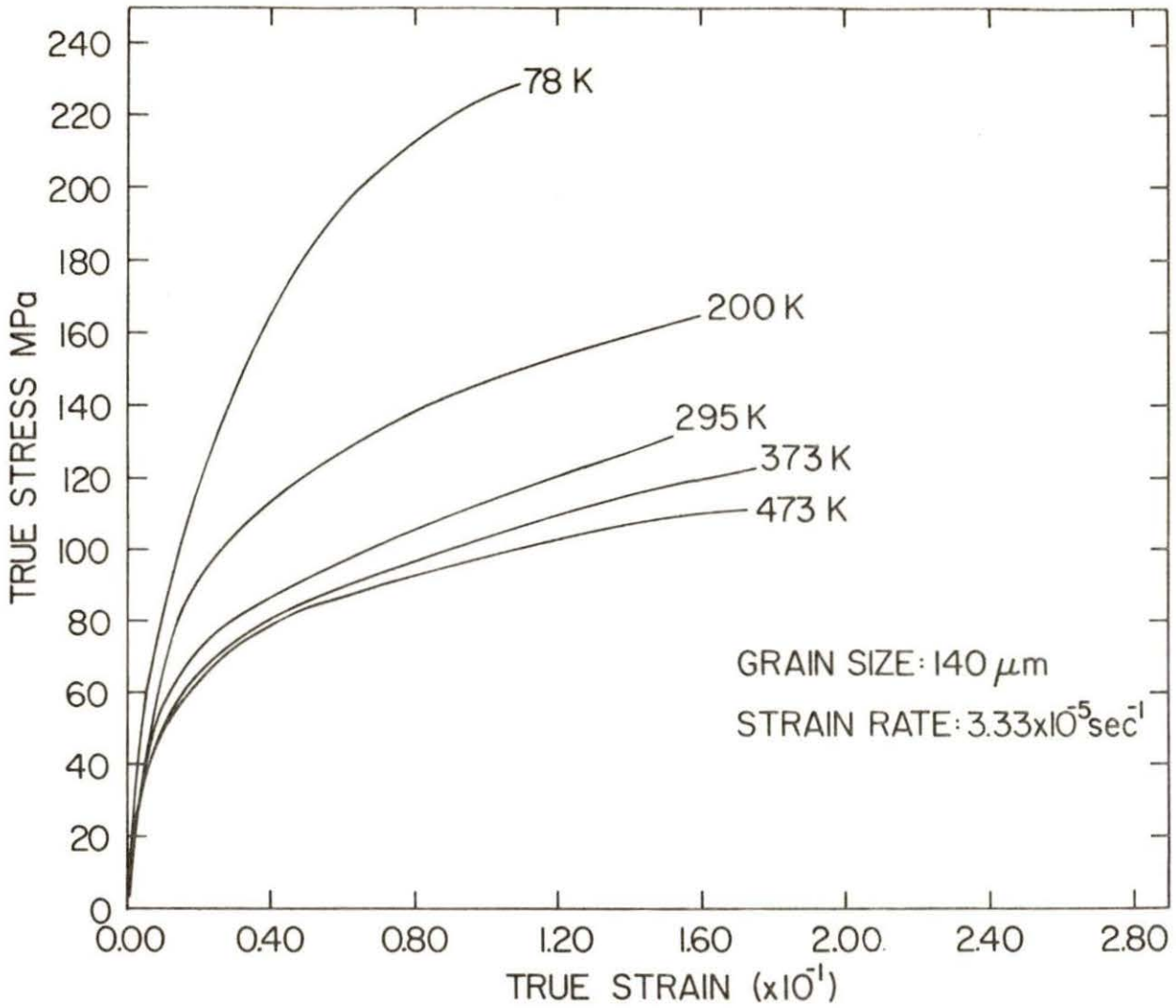

Fig. 2. True stress versus true strain for 140 μm grain size at various temperatures

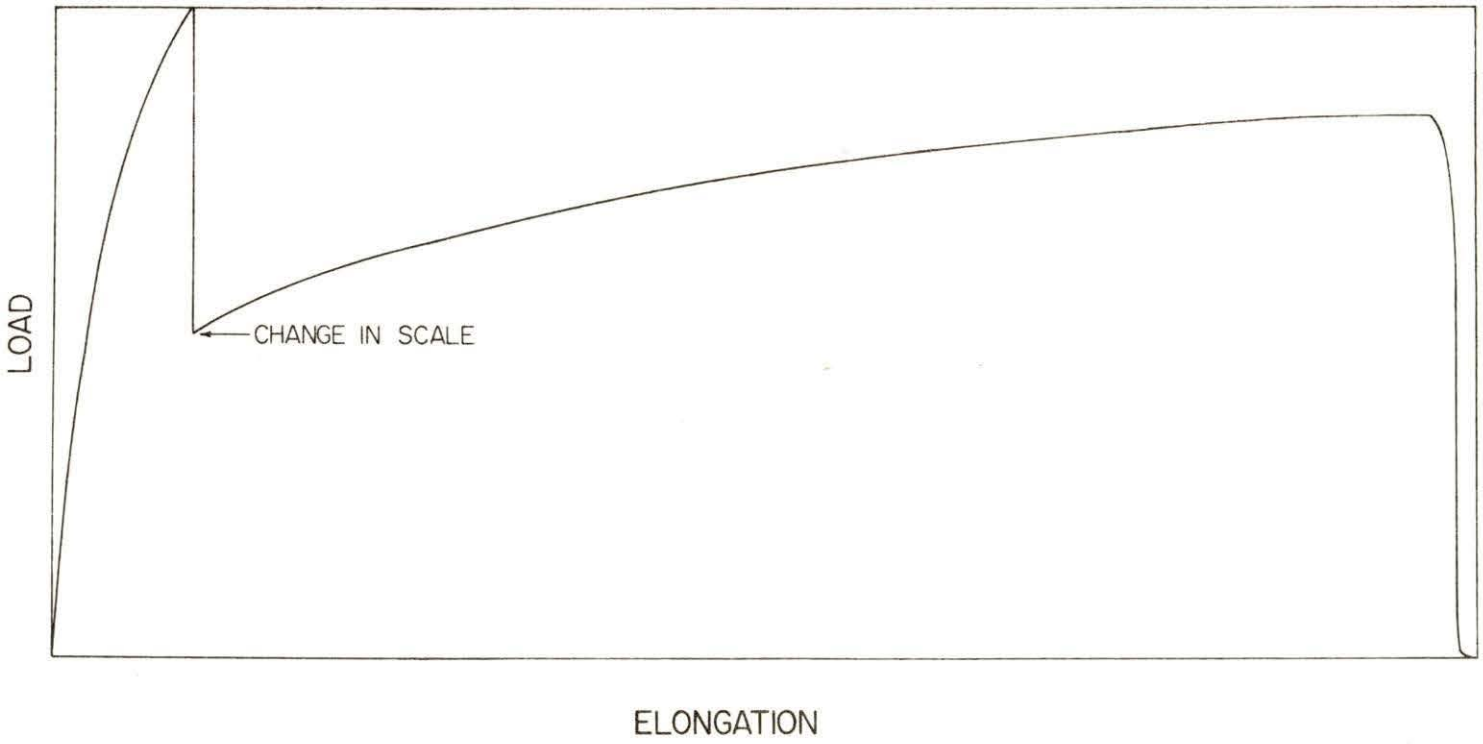

Fig. 3. Representative load-elongation curve

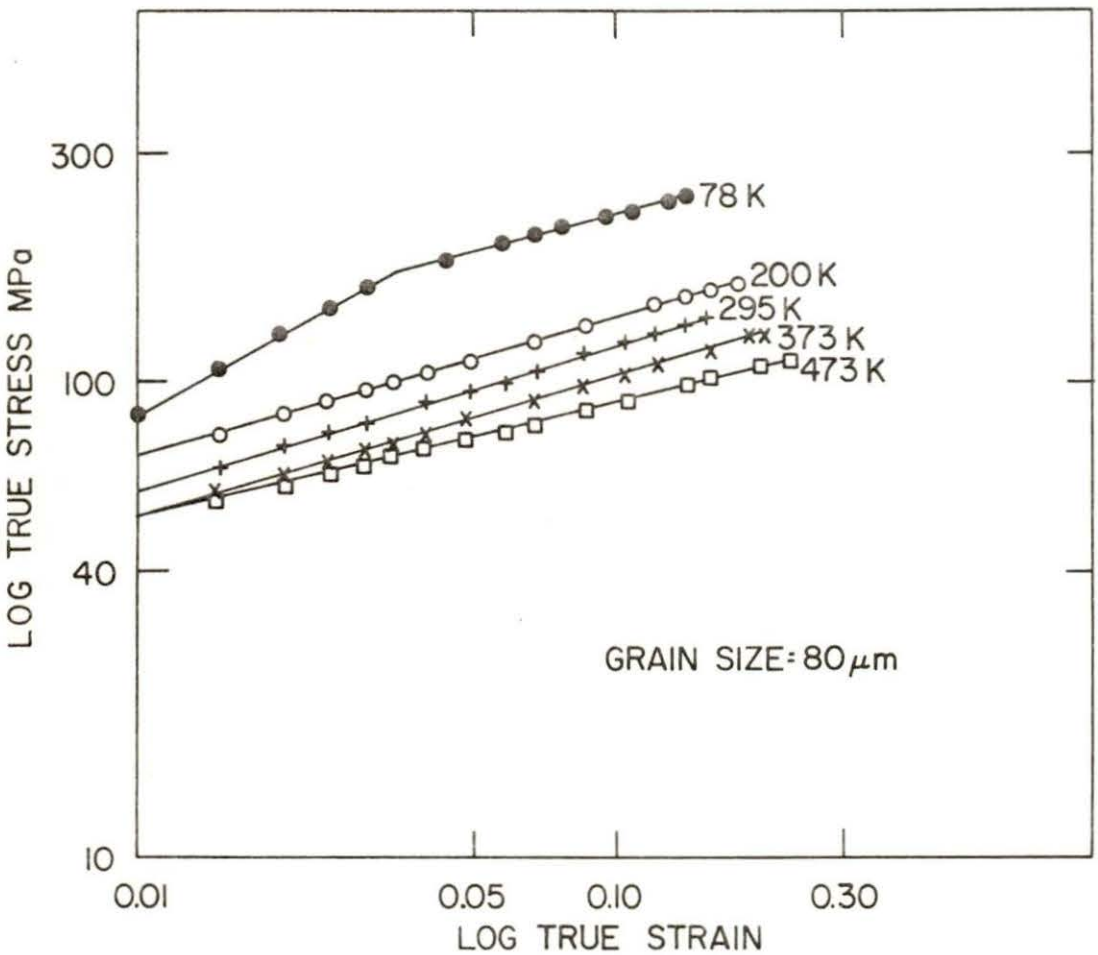

Fig. 4. Log true stress versus log true strain for 80 μm grain size at various temperatures

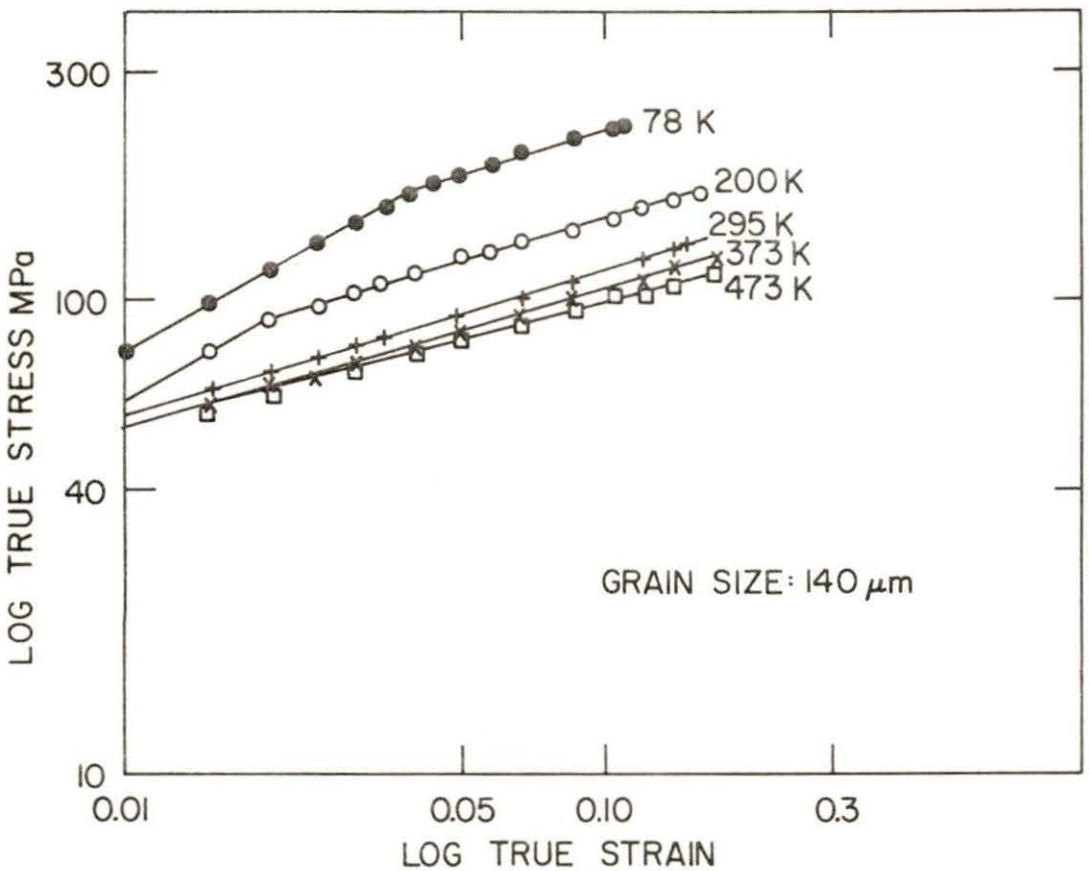

Fig. 5. Log true stress versus log true strain for 140 μm grain size at various temperatures

it is possible to represent the stress-strain behavior by a relationship of the form $(\sigma-\sigma_t) = K(\varepsilon-\varepsilon_t)^n$, where σ_t and ε_t represent the true stress and true strain at a true strain of 0.03, K is the strength coefficient and n is the work hardening exponent for that particular region. However, no simple relation or combination of simple relations can describe the stress-strain behavior over the full plastic range. The strain hardening exponents obtained from the slopes of the upper strain region are shown as a function of temperature in Fig. 6. The average values show a slight decrease in strain hardening rate with increasing test temperature above 373 K.

Temperature Dependence of the Flow Stress

The flow stress of scandium at several plastic strains is shown as a function of test temperature in Figs. 7 and 8. The flow stress at lower strains shows a small degree of temperature dependence, whereas at higher strains the flow stress increased at a faster rate with decreasing temperature. In previous studies of rare earth elements (8,9, 10,11,12) the temperature dependence of the flow stress was characterized by the following relation

$$\sigma_{(\varepsilon)} = \sigma_\beta \exp(-BT) \qquad (8)$$

where $\sigma_{(\varepsilon)}$ = true stress at a given stain.

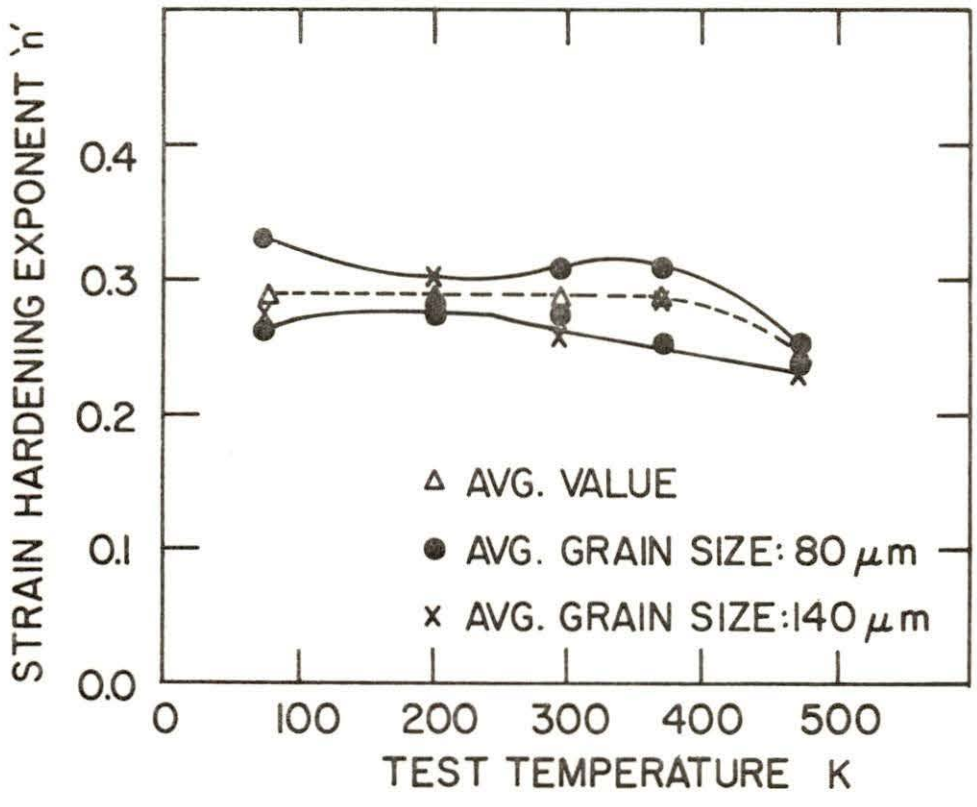

Fig. 6. Temperature dependence of the strain hardening exponents for 80 μm and 140 μm grain sizes

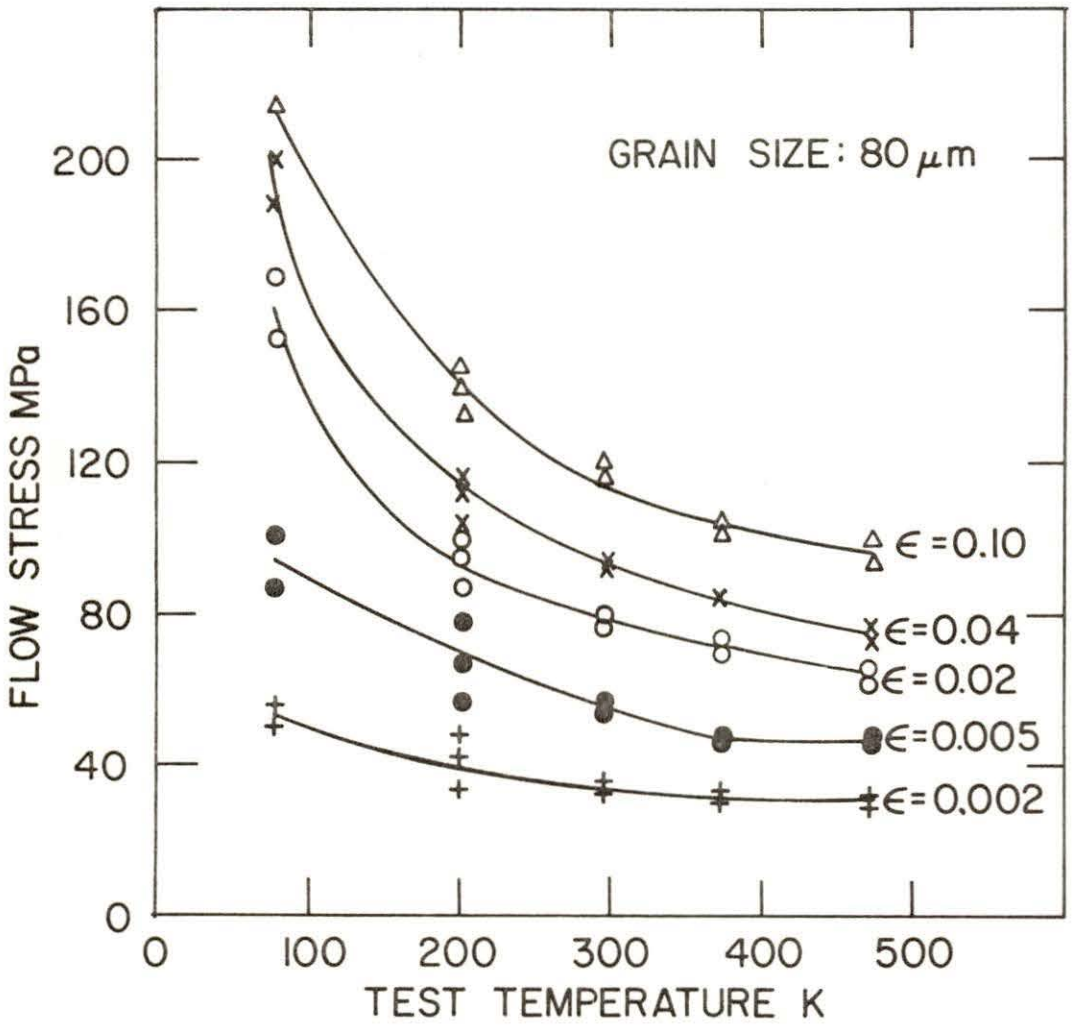

Fig. 7. Temperature dependence of the flow stress for 80 μm grain size at various strains

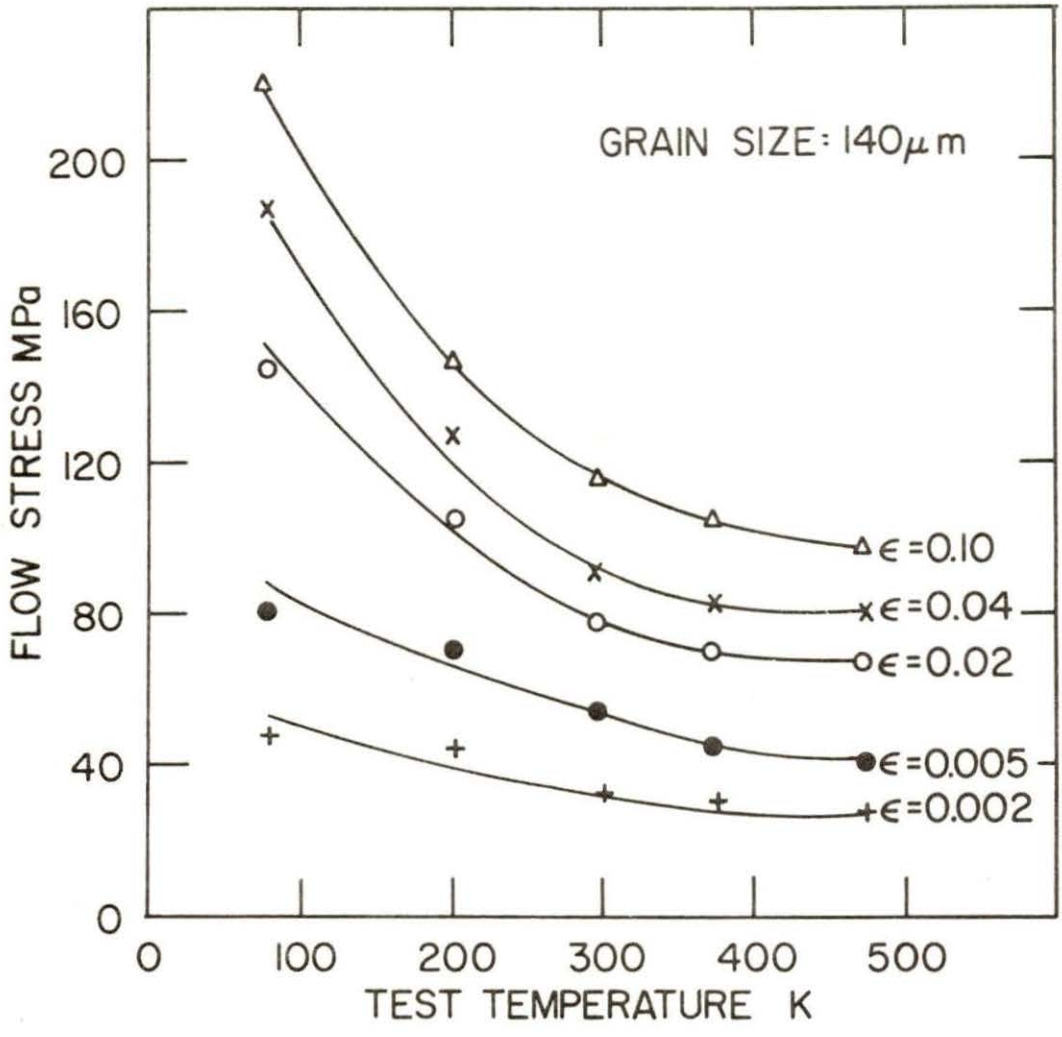

Fig. 8. Temperature dependence of the flow stress for 140 μm grain size at various strains

From Fig. 9, where the log of flow stress is plotted as a function of temperature for 80 μm grain size material, it may be seen that the flow stress exhibits a single exponential temperature dependence between 78 K and 373 K at strains of 0.002 and 0.005. A change to a lower slope occurs between 300 K and 400 K. At higher strains there appears to be a change to a stronger temperature dependence near 175 K to 200 K and the very low temperature dependence observed at low strains either does not exist or it occurs at temperatures above 473 K.

The log of flow stress versus temperature for 140 μm grain size material is plotted in Fig. 10. A single exponential temperature behavior is evident between 78 K and 300 K and a change to a lower slope occurs between 300 K and 400 K.

Metallographic investigation of longitudinally sectioned fractured specimens failed to reveal any unsual effect of grain size. Twinning was observed at all temperatures but the density of twins decreased with increasing temperature. In general the twin morphology was lenticular but a few sheaf-like patches of what appear to be twins are observed in samples tested at 373 K and higher as shown in Fig. 11. In addition, uniformly distributed voids were formed in the gage section at all temperatures tested. Near the fracture surface the density of voids increased.

Strain-Rate Dependence

Strain-rate changes were performed at five temperatures using

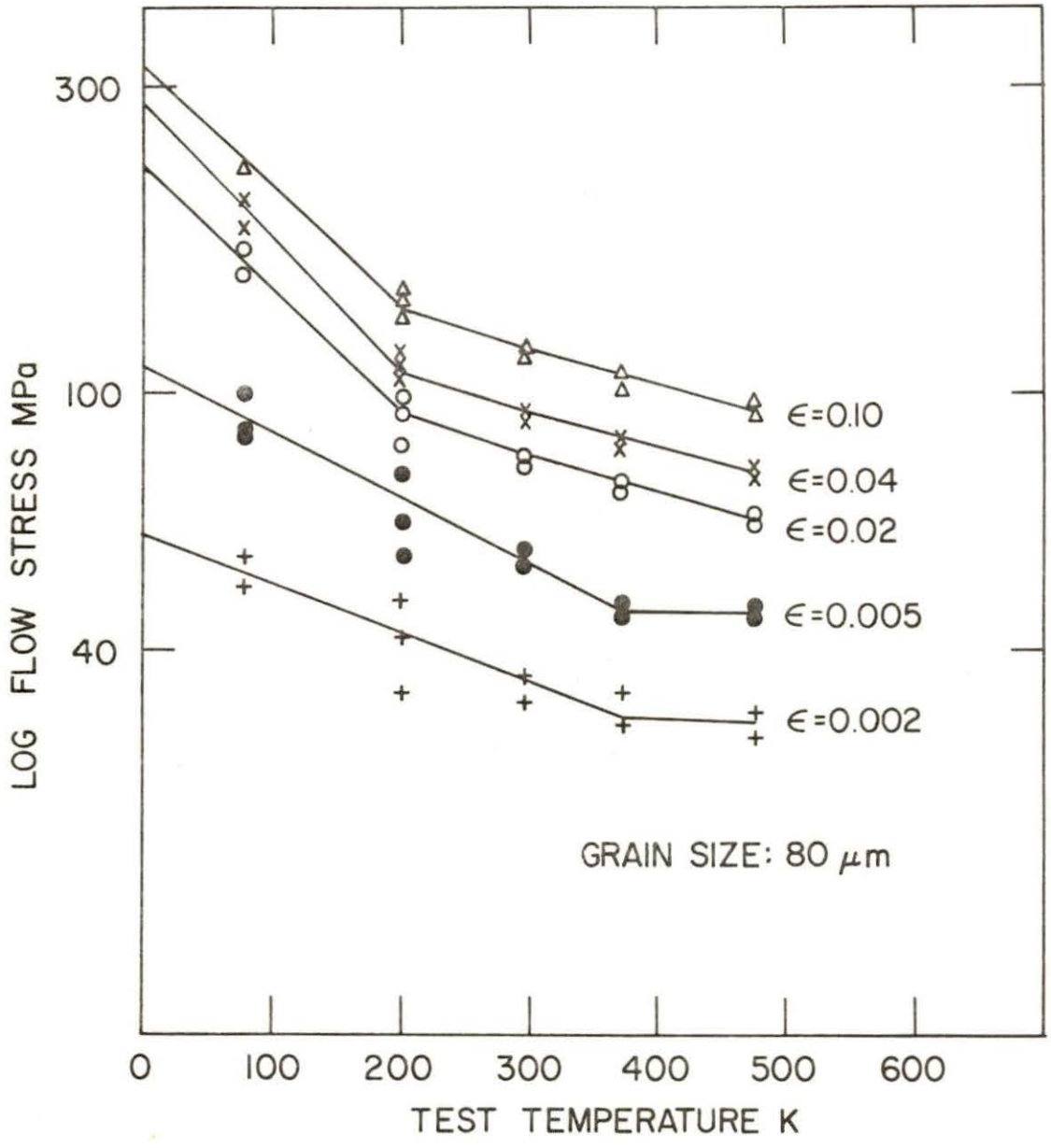

Fig. 9. Log flow stress versus temperature for 80 μm grain size

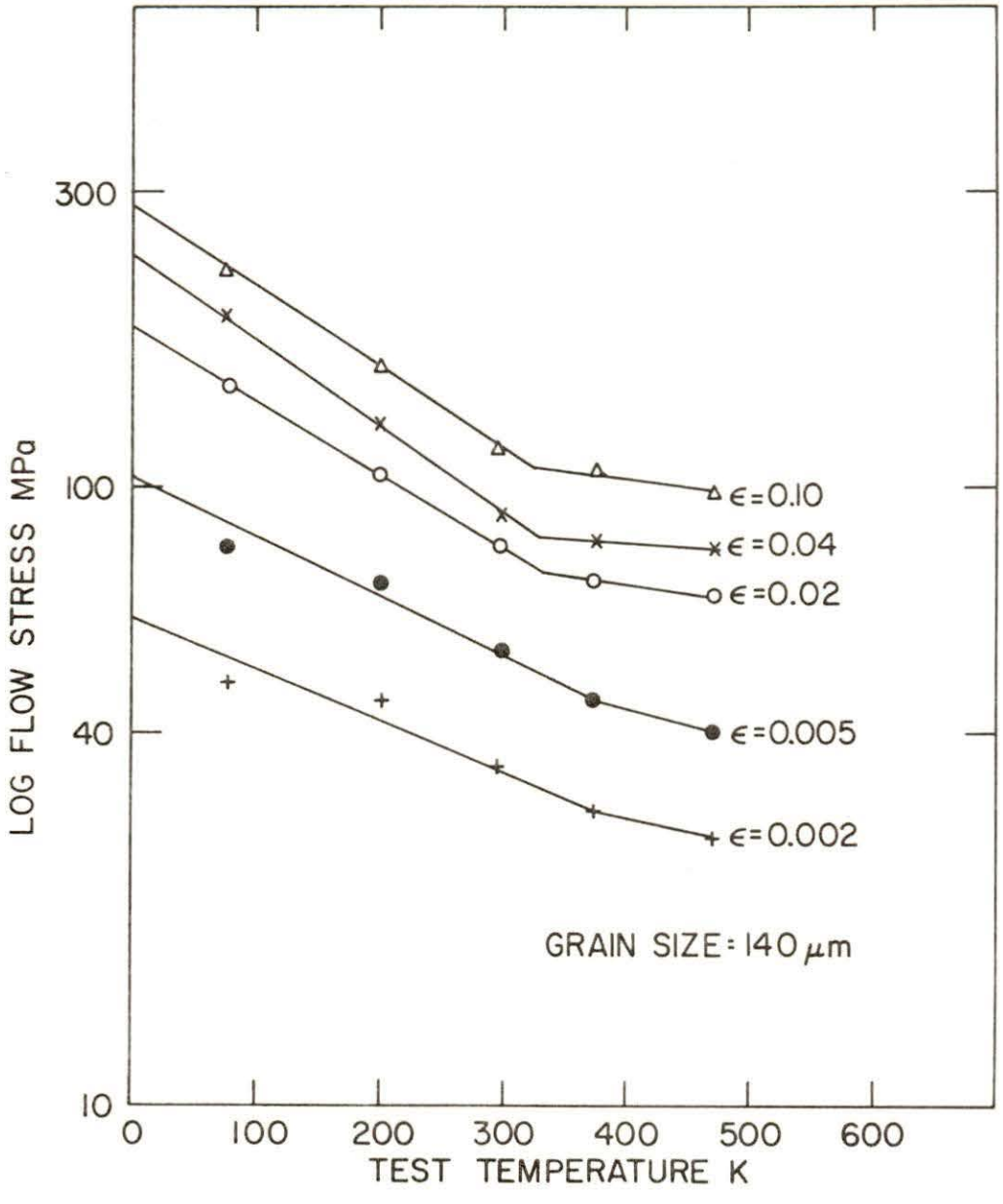

Fig. 10. Log flow stress versus temperature for 140 μm grain size

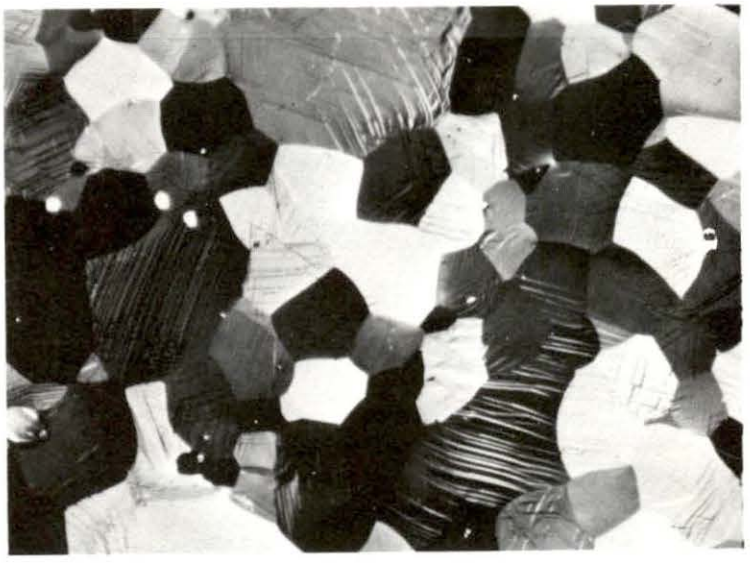

78 K 150X

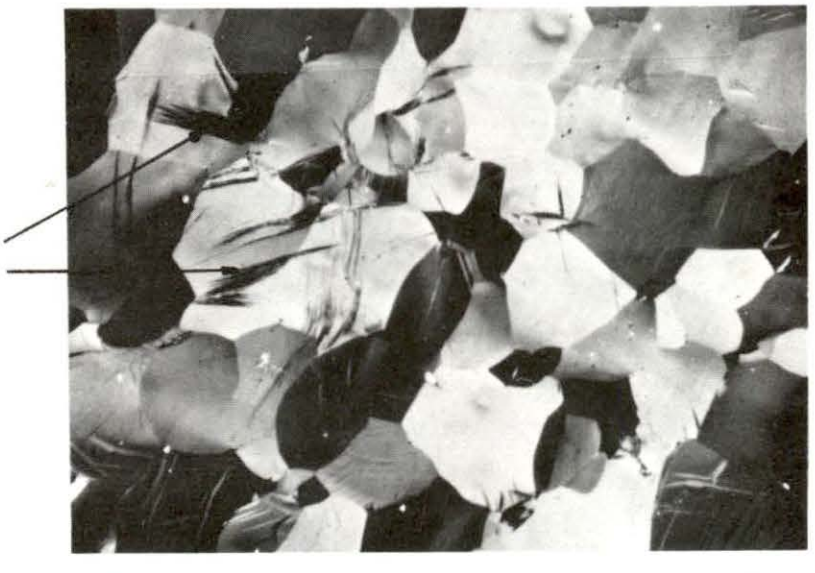

373 K 150X

Fig. 11. Photomicrograph illustrating the change of deformation twins from lenticular at 78 K to sheaf-like patches at 373 K. Arrows indicate sheaf-like patches. Note this change was only partial. (As electropolished in 6% perchloric acid 94% methanol at 200 K, polarized light)

140 μm grain size specimens. The strain rate sensitivity parameter, 'm', was determined by changing the strain rate by pushbutton control between the strain rates of 3.33×10^{-5} sec^{-1} and 3.33×10^{-3} sec^{-1} approximately every 1 percent strain during the course of a tensile test. The rate sensitivity parameter is plotted as a function of strain in Fig. 12. At strains greater than 0.06 the rate sensitivity is virtually independent of strain except at 295 K. The temperature dependence of the rate sensitivity at true strains of 0.04 and 0.12 are shown in Fig. 13. The rate sensitivity exhibited the common rise with increasing temperature to a maximum at about 250 K. However, rather than continuing to decrease with increasing temperature above the maximum, a second rise sets in near 350 K.

Ductility

Reduction of area at fracture and uniform elongation as a function of temperature are shown in Fig. 14. The overall trend appears to be a general increase in ductility with increasing temperature. It should be noted that the range of values reported on Fig. 14 include both the 80 μm and 140 μm grain size data.

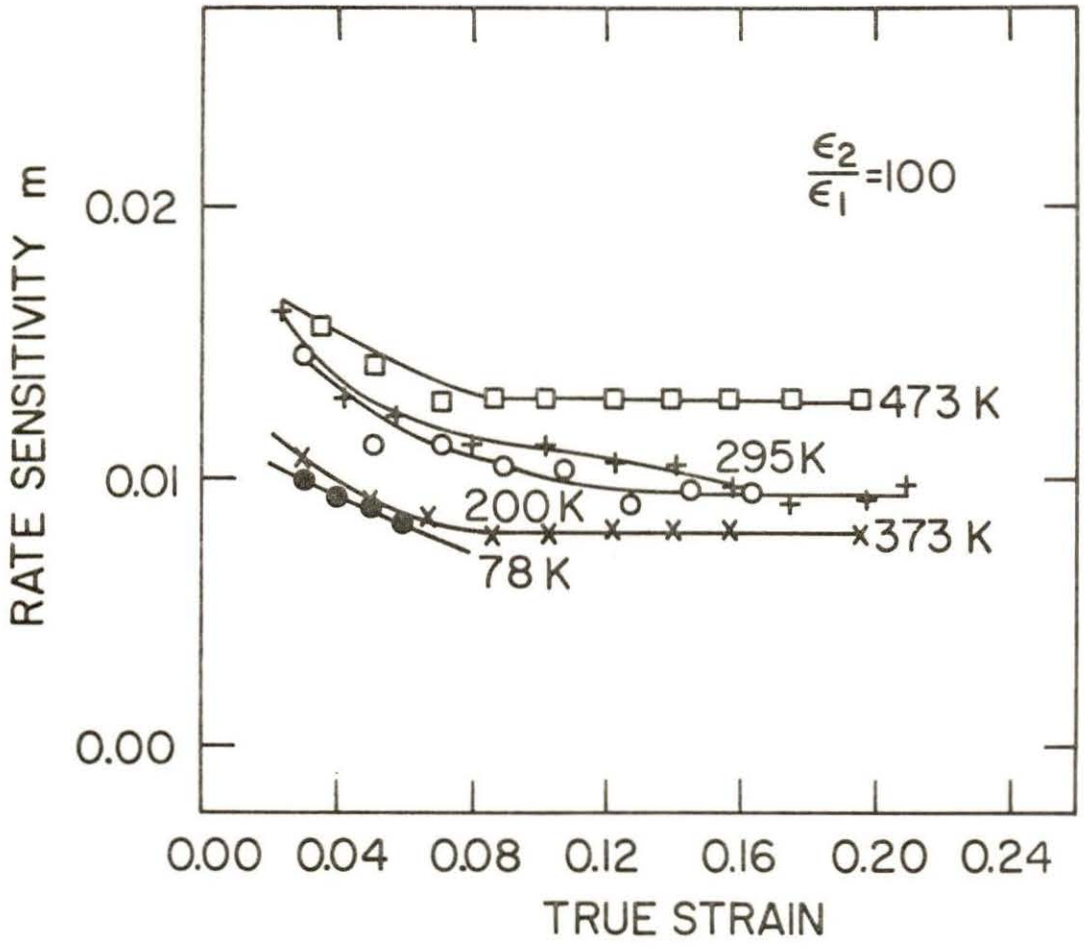

Fig. 12. Plot of rate sensitivity as a function of strain for several test temperatures

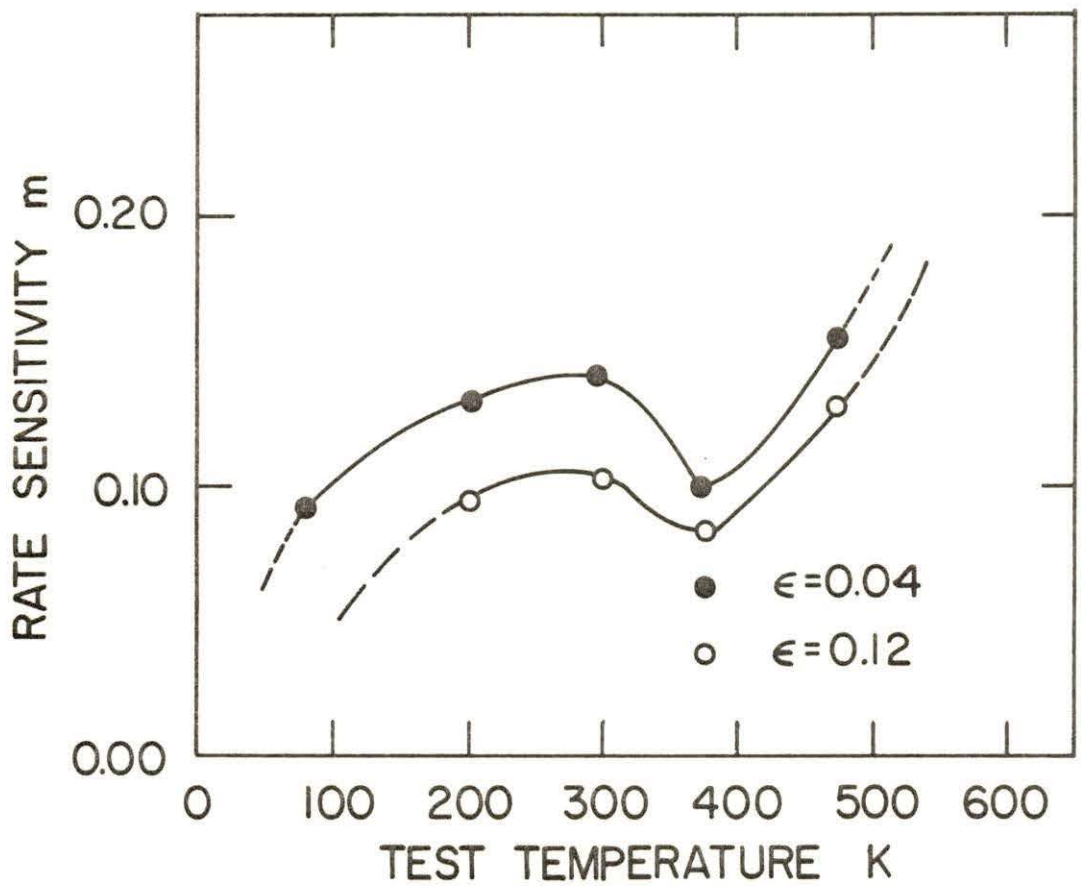

Fig. 13. Temperature dependence of the rate sensitivity at 4% and 12% strain

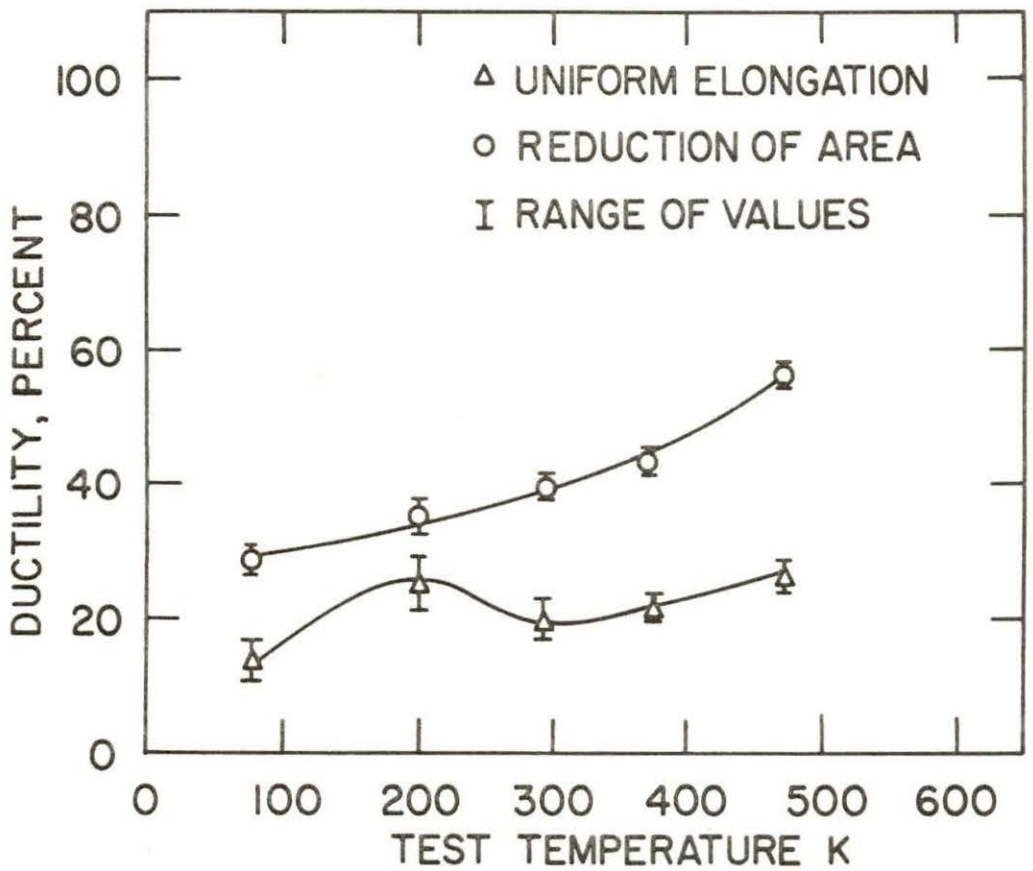

Fig. 14. Plot of uniform elongation and reduction of area as a function of temperature. Average values with range are shown

DISCUSSION

In Figs. 15 and 16 the ultimate tensile strength and ductility, respectively, from previous studies (13) and the present one are summarized. In the overlapping test temperature range the ultimate tensile strength of the "purer" scandium decreased with increasing test temperature, whereas previous results revealed an increase followed by a decrease with increasing test temperature. The increase in tensile strength in the previous scandium studies was attributed to dynamic strain aging (13). The ductility of the "purer" scandium, as measured by percent uniform elongation and reduction in area, increased with increasing test temperature and was greater than obtained in previous studies.

In general, the mechanical behavior of scandium has been found to be comparable with other HCP heavy rare-earth metals (yttrium, erbium, dysprosium, gadolinium, and samarium) that have been investigated (8,9, 10,11,12). Below 300 K, the strength decreases with increasing test temperature. However, at temperatures above 300 K humps attributed to dynamic strain aging were observed when the log of flow stress versus temperature was plotted. In yttrium (8), which has a melting temperature similar to that of scandium, the stress hump tended to begin at 300 K, whereas in scandium an upward deviation of the flow stress from single exponential temperature dependence tends to begin near 373 K. However, it is not clear that this behavior reflects the onset of a stress hump. It should be noted that the higher total interstitial impurity content of yttrium could promote the onset of dynamic strain aging at a lower

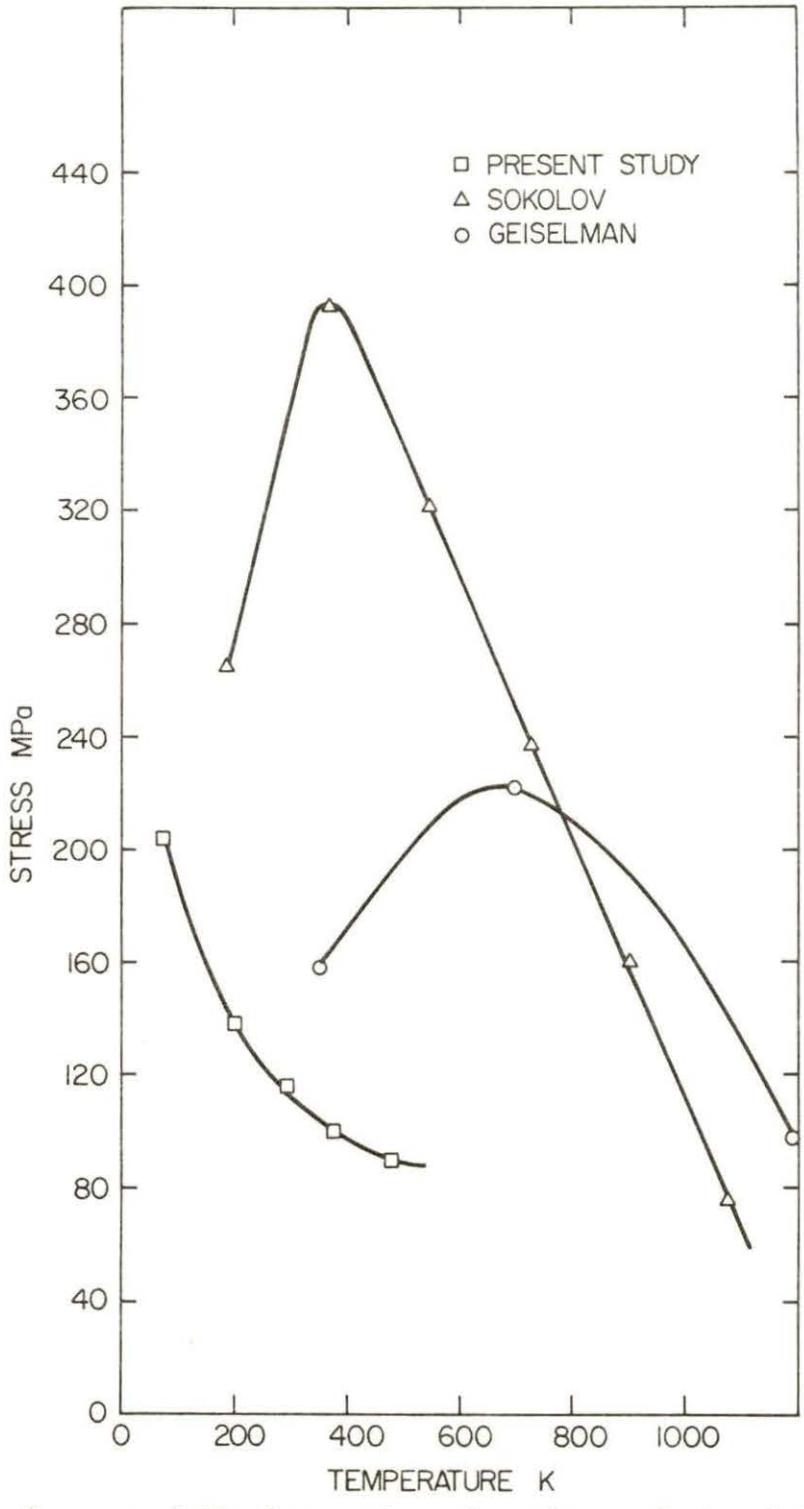

Fig. 15. Summary of the temperature dependence of the ultimate tensile strength from previous studies (13) and the present investigation

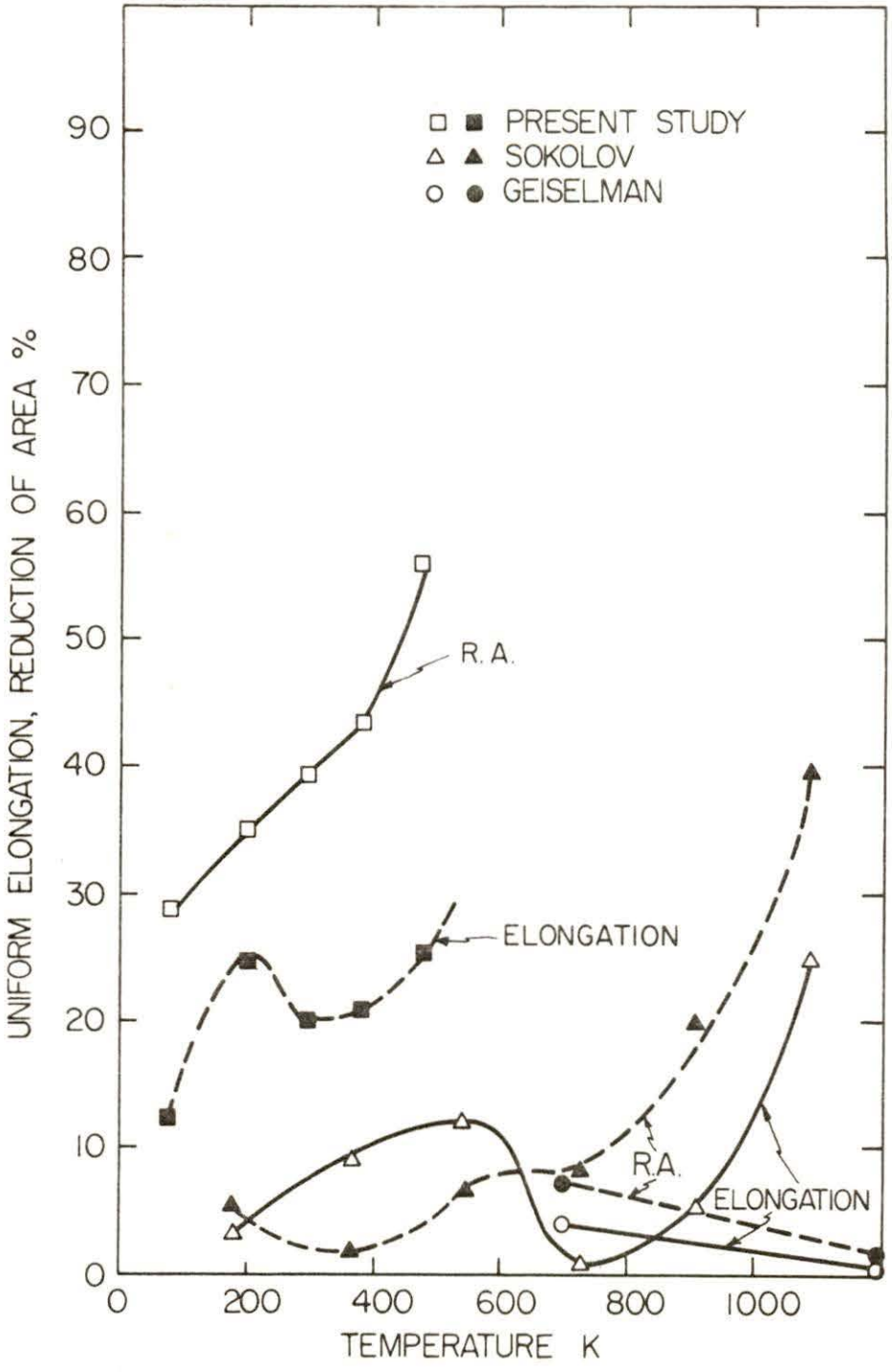

Fig. 16. Summary of the temperature dependence of the ductility parameters from previous studies (13) and the present investigation

temperature.

Information leading to possible deformation mechanisms in pure metals can be obtained from strain-rate change tests at constant temperature. The most direct way of determining whether one or more rate-controlling mechanism is operative would be to determine the variation of activation volume as a function of effective stress. If the results would fit a single curve, that would be a strong indication of a single rate-controlling mechanism. In addition, Conrad (14) used the activation volume values to identify tentatively the rate-controlling mechanism.

The activation volume as a function of strain and stress are plotted in Figs. 17 and 18, respectively. Before discussing further the main features of Figs. 17 and 18, it should be emphasized that the activation volume calculated in this work is a pseudo-activation volume because the Taylor factor (M) used in converting true stress to shear stress is not well defined for hexagonal close packed structures. A review of the literature revealed a range of Taylor factors varying between 2 and 6 (15, 16, 17). In addition, the activation volume is commonly plotted against the effective stress. Since it was not possible to select with reasonable certainty an athermal region of the flow stress, the total stress is plotted in Fig. 18. This also could not be converted to shear stress because the Taylor factor is unknown.

From Fig. 17 it can be seen that the pseudo-activation volume is relatively strain independent at lower temperatures, but tends to decrease with increasing strain at higher temperatures. The pseudo-activation volume is plotted against the total stress for various

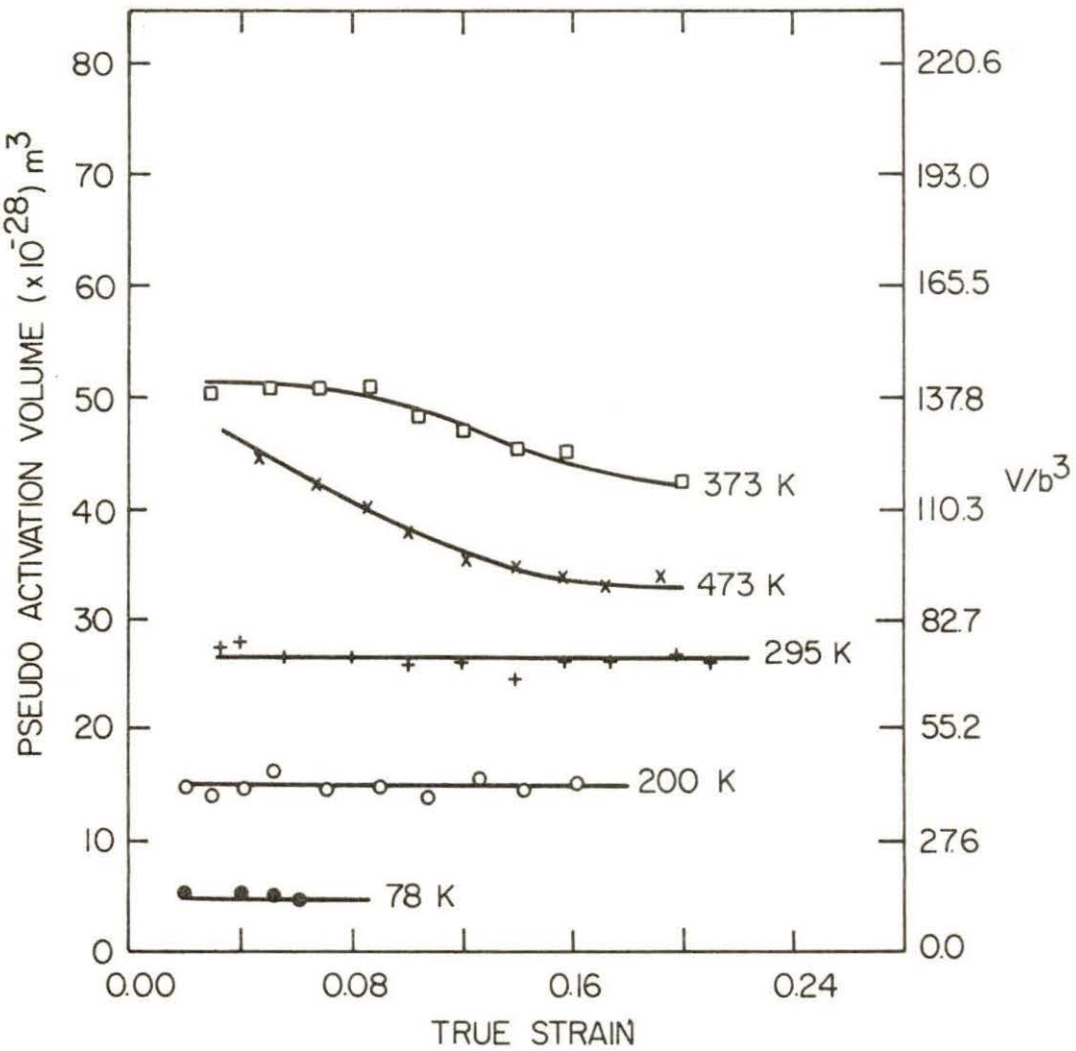

Fig. 17. Pseudo-activation volume versus strain. The value of b used in b^3 was 3.31×10^{-10} m (1, p. 77)

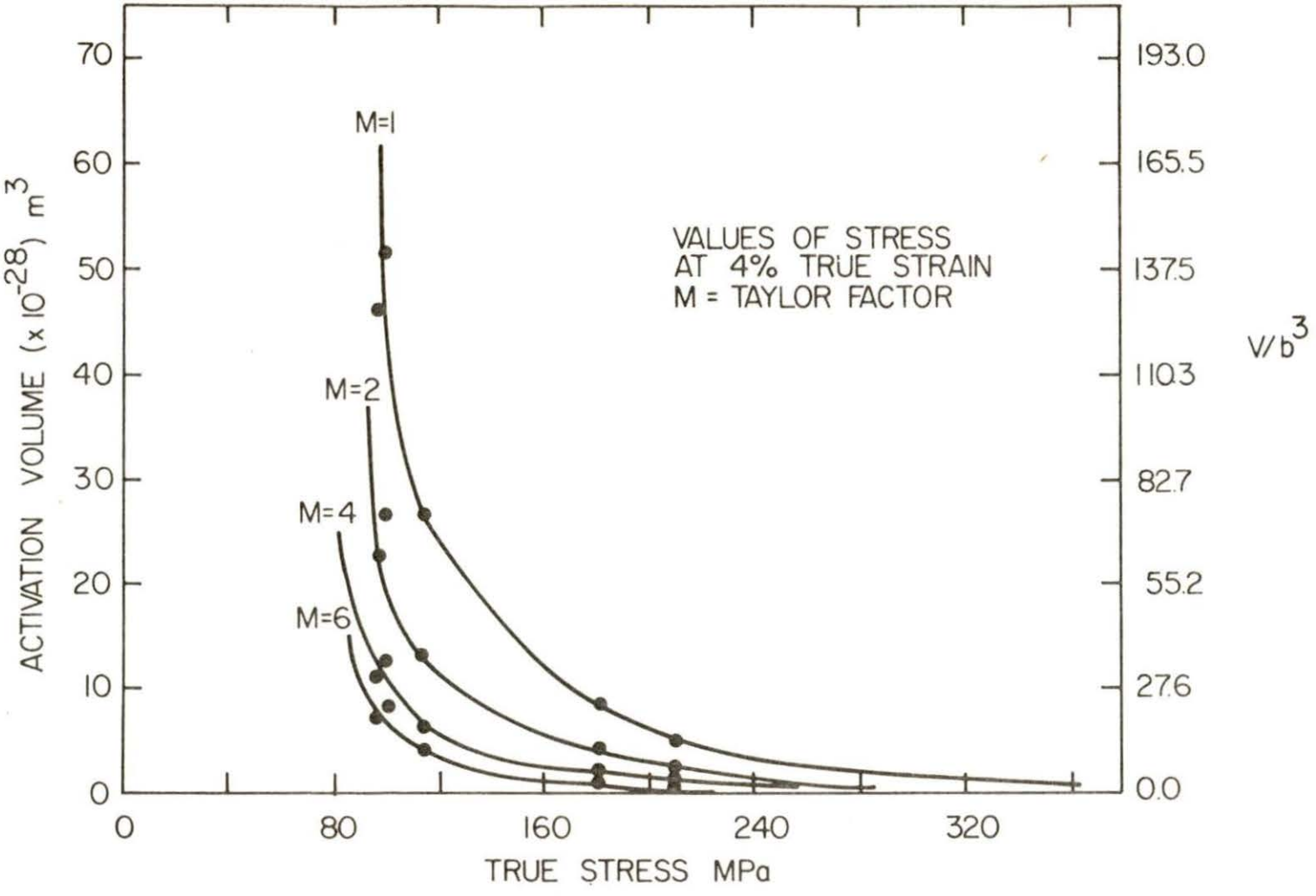

Fig. 18. Activation volume versus stress for various Taylor (M) factors. Stress values were taken at 4% true strain

Taylor factors in Fig. 18. The activation volume was low and nearly independent of stress in the high stress region. Furthermore, the literature shows numerous examples of activation volume data for HCP metals, plotted against effective stress that conform closely to the shape of the curve obtained in this investigation.

The observed activation volume results suggest that a single deformation mechanism is operative in the range of temperatures used in this investigation. Furthermore, if a value of three is used for the Taylor factor, it can be seen that the activation volume varied from 7.0 b^3 to 62.0 b^3. According to a summary by Conrad (15), the values of activation volume cited above are consistent with the following possible rate controlling mechanisms; overcoming the Peierls stress, cross slip, or overcoming impurity atoms.

There have been numerous studies on the mechanical properties and rate-controlling mechanisms in zirconium (16,17) and titanium (18,19). These studies were conducted at high enough temperatures to determine an athermal stress value, i.e. the stress value at which the flow stress becomes nearly independent of temperature, thus determining the thermal component of stress and and the deformation mechanism. In the range of temperatures used in this investigation the mechanical behavior of titanium and zirconium was very similar to that of scandium. The activation volumes obtained were independent of stress at low temperatures and varied from 10 b^3 to 140 b^3. Moreover, it was found that the ther-

mally activated overcoming of impurity atoms was the rate-controlling mechanism for deformation in Ti and Zr. Therefore it is expected that in scandium the overcoming of residual impurity atoms is the rate-controlling mechanism of deformation.

CONCLUSION

The stress-strain characteristics, flow stress behavior and strain rate sensitivity were determined for "pure" scandium over the temperature range of 78 K to 473 K. The following conclusions may be extracted from the results of this investigation:

(1) The overall behavior of scandium is very similar to that of other HCP heavy rare-earth elements that have been investigated by Owen and Scott (9,10,11,12).

(2) The strength of Sc was considerable lower and the ductility higher when compared to previous studies (4,6).

(3) The flow stress was found to deviate from a single exponential temperature dependence near 373 K. However it is not clear whether this behavior reflects the onset of dynamic strain aging found in studies of HCP heavy rare-earth metals.

(4) At low temperatures the pseudo-activation volume is independent of strain and stress suggesting that overcoming of residual impurity atoms might be the rate controlling deformation mechanism in scandium.

PART II. HYDROGEN EMBRITTLEMENT OF SCANDIUM

INTRODUCTION

The presence of hydrogen in metals in excess of the terminal solid solubility can result in the precipitation of metal hydrides. Experiments have shown that hydrogen embrittlement, as measured by the loss in ductility, can be attributed to presence of hydrides in the metal matrix (20, 21,22,23,24), to stress induced hydrides (25,26,27), or to hydrogen in solution (28,29,30). The large terminal solid solubility of hydrogen in scandium at low temperatures, approximately 33 at% H (1, p. 155), provides an opportunity to determine unequivocally whether hydrogen embrittlement can occur in hydride-forming metals at concentrations below the solubility limit.

Hydrogen embrittlement research on hexagonal close packed (HCP) metals has been confined primarily to titanium and zirconium (22,24,25, 31,32), because of their extensive industrial use. These metals exhibit high terminal hydrogen solid solubilities at elevated temperatures, but at 295 K the solubility is less than 0.5 at% H in both metals. Consequently hydrogen embrittlement of Zr and Ti at low temperatures has been attributed to stress induced hydrides or to the presence of hydrides in the metal matrix.

The scandium-hydrogen phase diagram (1 p. 158) shown in Fig. 1 shows that up to 33 at% H can be held in solid solution at 295 K and that the solubility increases to 39 at% H at 1273 K. Lattice constant measurements of scandium-hydrogen alloys by Azarkh and Funin (33) and pressure-composition data reported by Stampfer (34) and Lieberman and Wahlbeck (35) are

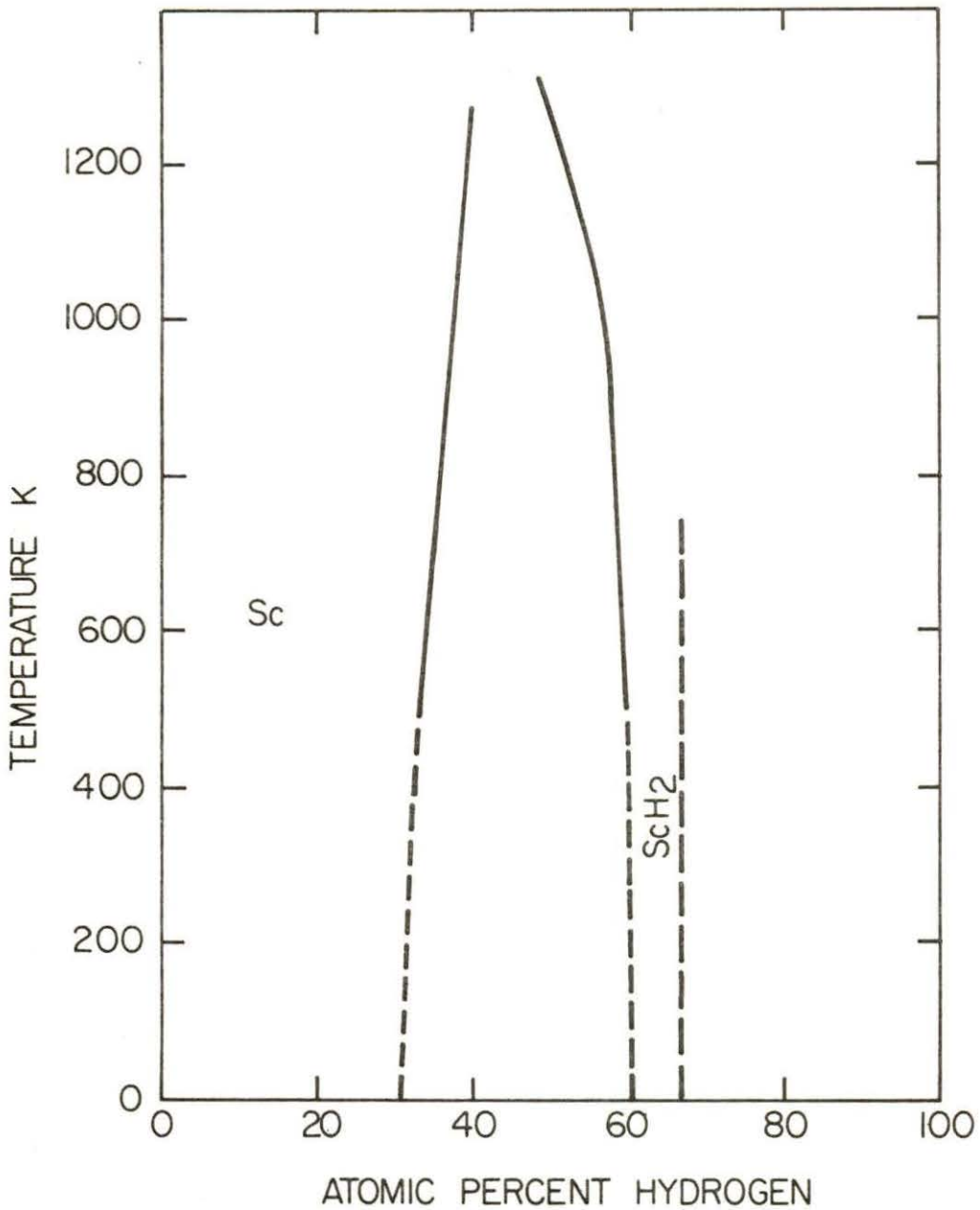

Fig. 1. Scandium-hydrogen phase diagram

in good agreement with each other for the Sc/Sc + ScH_2 phase boundary. Recent electrical resistivity measurements by Jensen and Zalesky (36) on the scandium-hydrogen alloys employed in the present investigation have shown that 20.83 at% H can be held in solid solution at 4.2 K.

MATERIALS AND PROCEDURE

The fabrication and the tensile testing procedures employed have been described earlier. Hydrogen charging of all samples was done thermally by heating the specimens to 1023 K for 80 min under a dynamic vacuum of 1.33×10^{-5} Pa to recrystallize and anneal the specimens. The chamber was then isolated from the vacuum system and high purity hydrogen from the thermal decomposition of uranium hydride was admitted at predetermined pressures and the closed system was held at 1023 K for an additional 40 min. Samples of a given composition were then wrapped in zirconium sheet and sealed in a quartz tube under vacuum for further heat treatment designed to insure a homogeneous hydrogen distribution. Thermal treatment consisted of placing the quartz tubes in a furnace maintained at 1130 K for 135 min before furnace cooling. Uniform hydrogen distribution was verified by hot vacuum extraction analysis of segments taken from each end of samples. Chemical analyses of the various scandium-hydrogen alloys after tensile testing are shown in Table 1. Grain size determinations were performed on several samples using the intercept method (7). The results showed grains of varying size, with an average diameter of 140 μm. In addition, a sample containing hydrogen in excess of the solid solubility (34.6 at% H) was prepared to obtain information about the morphology of scandium hydride.

The tensile testing temperatures employed were 78, 200, 295, 373, and 473 K. All tests were run at a strain rate of 3.33×10^{-5} sec^{-1}.

Strain rate sensitivity measurements as well as tensile tests at a higher strain rate were conducted on scandium containing 14.14 at% H. The strain rates employed were 3.33×10^{-5} sec^{-1} and 3.33×10^{-3} sec^{-1}, whereas the higher strain rate employed was 3.33×10^{-2} sec^{-1}.

Samples were cut from the grip section of the hydrogen charged tensile specimens after tensile testing and were mounted in copper blocks for visual hydride precipitation determination at low temperatures. Metallographic examinaton was done on the inverted stage microscope described by Sherman et al. (30).

Table 1. Interstitial solute content of tensile samples[a], ppm by weight

Samples	Hydrogen	Oxygen	Nitrogen	Remarks
As worked	48±8	140±52	7±4	20 samples
MZ-Sc A	486±22	180±37	18±8	5 samples
MZ-Sc B	2160±114	196±37	26±4	5 samples
MZ-Sc E	3678±192	208±84	56±16	13 samples
MZ-Sc C	4660±102	234±91	108±77	5 samples
MZ-Sc D	5863±277	547±85	485±124	5 samples

[a]Analyzed after testing. H, O, and N by vacuum fusion.

EXPERIMENTAL RESULTS

True stress-true strain curves at 78 K, 295 K, and 473 K for all hydrogen concentrations employed are shown in Figs. 2 through 4, respectively. These curves are plotted to maximum load; however, the amount of unloading preceding fracture was minimal in most instances. Exceptions to this load-elongation behavior occurred in alloys containing 17.27 and 20.83 at% H tested at 473 K as shown in Fig. 5 by the extensive elongation beyond maximum load.

Although the addition of 2.12 at% H decreased the strength of scandium in the range of test temperatures used, the yielding characteristics remained similar to those of scandium. However, strengthening occurred at higher hydrogen concentrations. From the insert in Fig. 3, it can be seen that scandium containing 20.83 at% H exhibited a large yield drop. The temperature and concentration dependence of well defined yield drops are illustrated in Fig. 6 where the open circles reflect the absence and solid circles the presence of a yield drop. At temperatures below 473 K the onset of yielding is strongly temperature and concentration dependent.

The strain hardening exponents obtained from the slopes of the higher strain ($\varepsilon>0.02$) region of the log true stress versus log true strain plots shown in Figs. 7 through 9, are summarized in Fig. 10 where the curves delineate the upper and lower bounds of the data. Two features of strain hardening behavior can be noted. At test temperatures below 295 K, the strain hardening rate is increased by hydrogen additions and a sharp

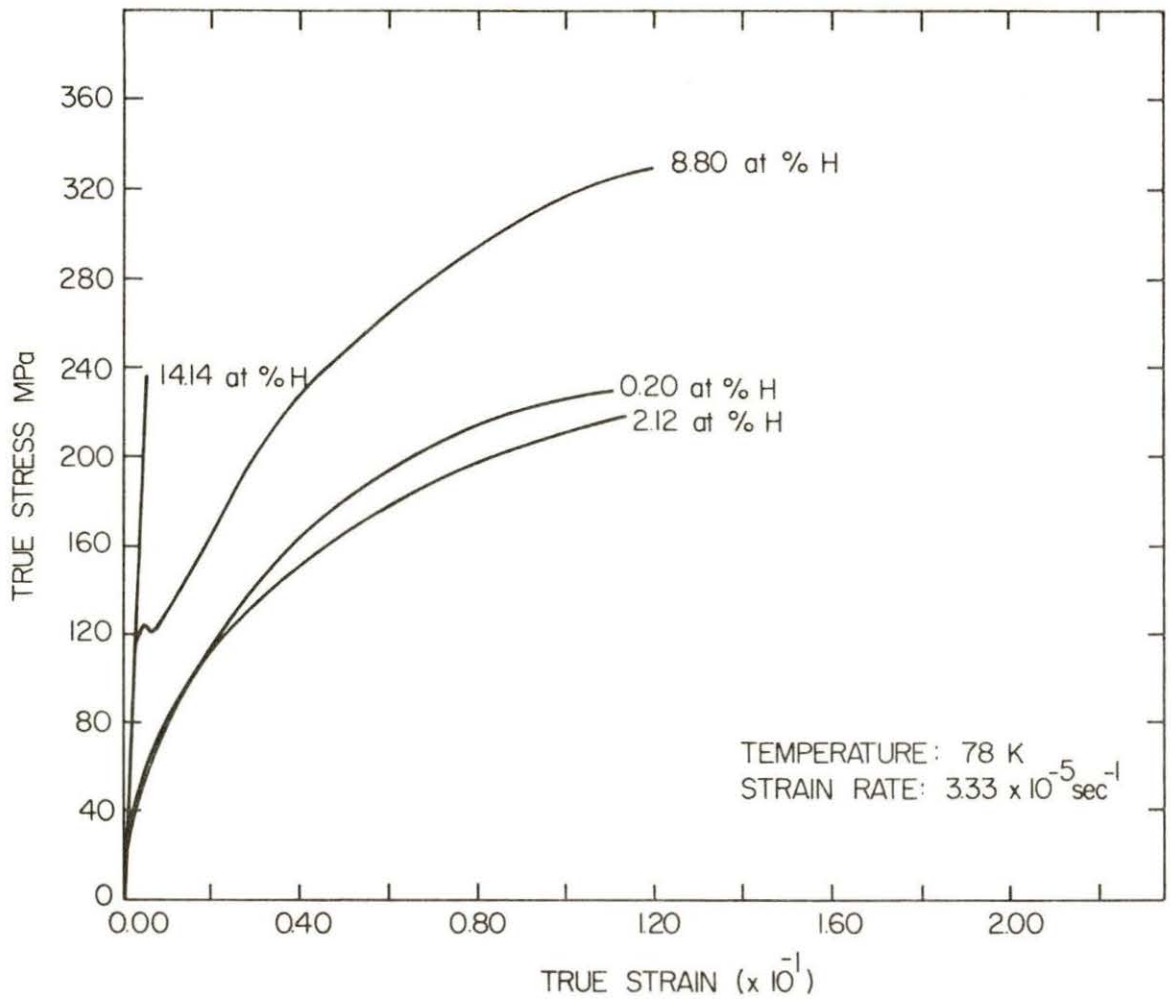

Fig. 2. Stress-strain plots for scandium-hydrogen alloys tested at 78 K

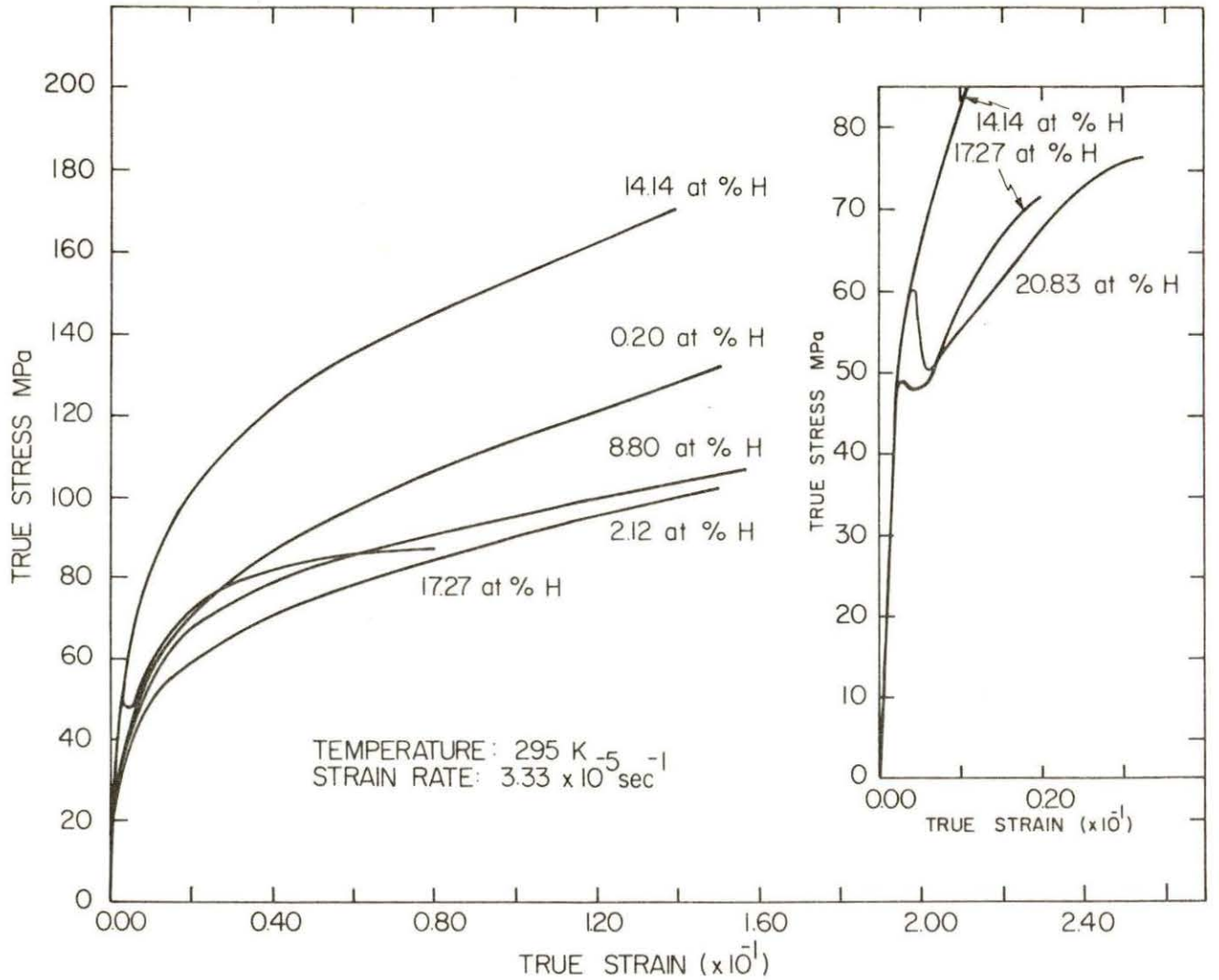

Fig. 3. Stress-strain plots for scandium-hydrogen alloys tested at 295 K

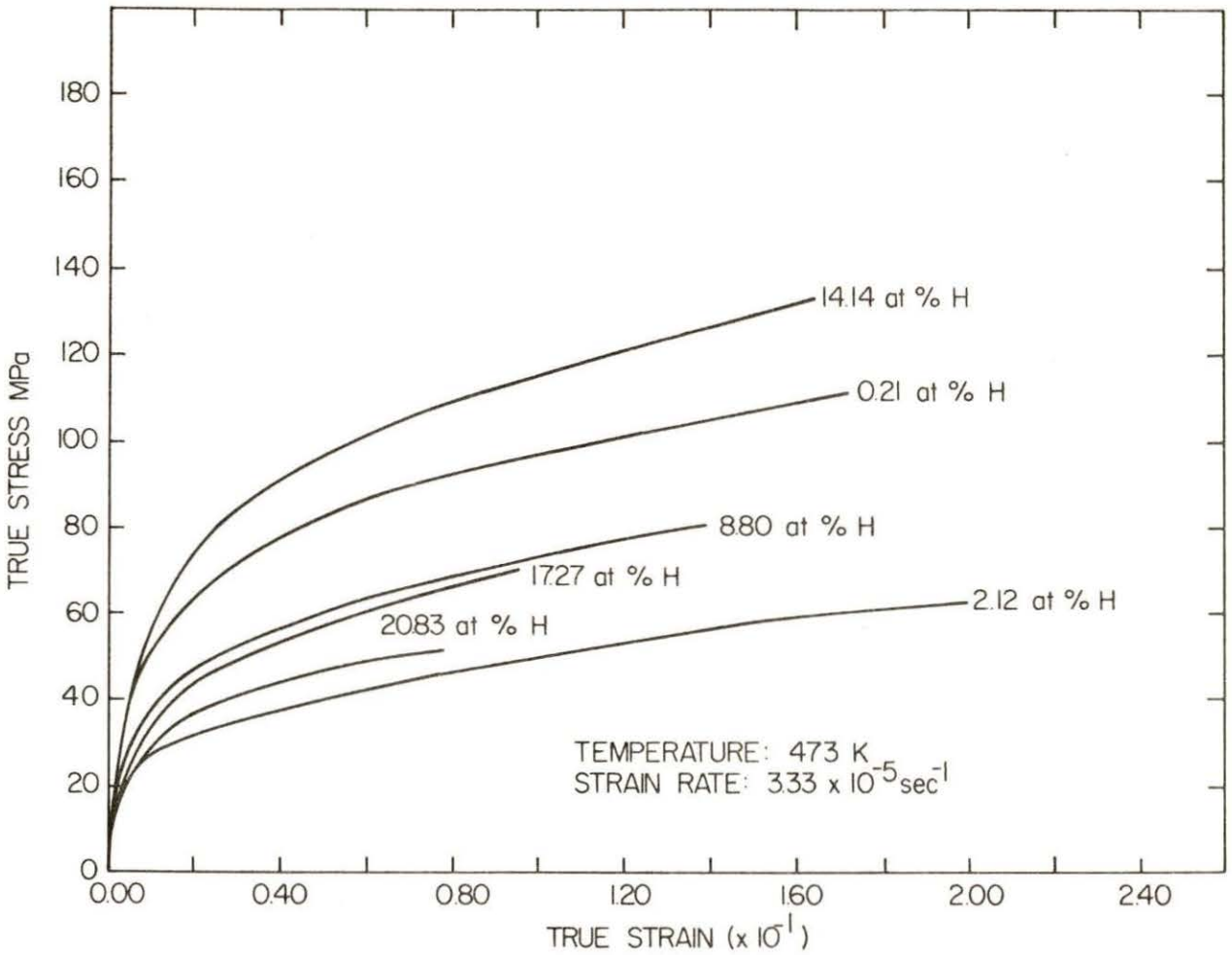

Fig. 4. Stress-strain plots for scandium-hydrogen alloys tested at 473 K

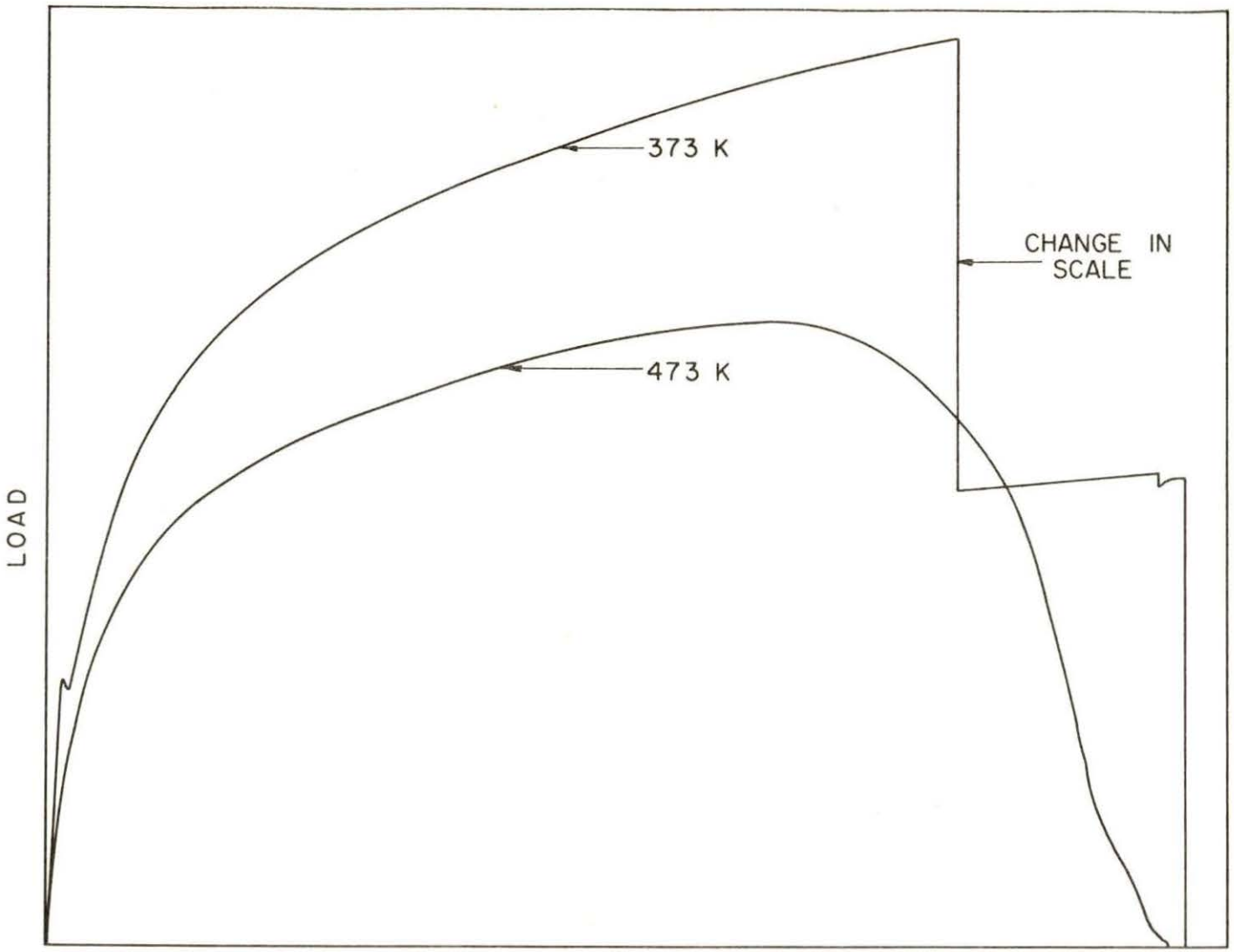

Fig. 5. Load-elongation curves for scandium containing 20.83 at% H tested at 373 K and 473 K

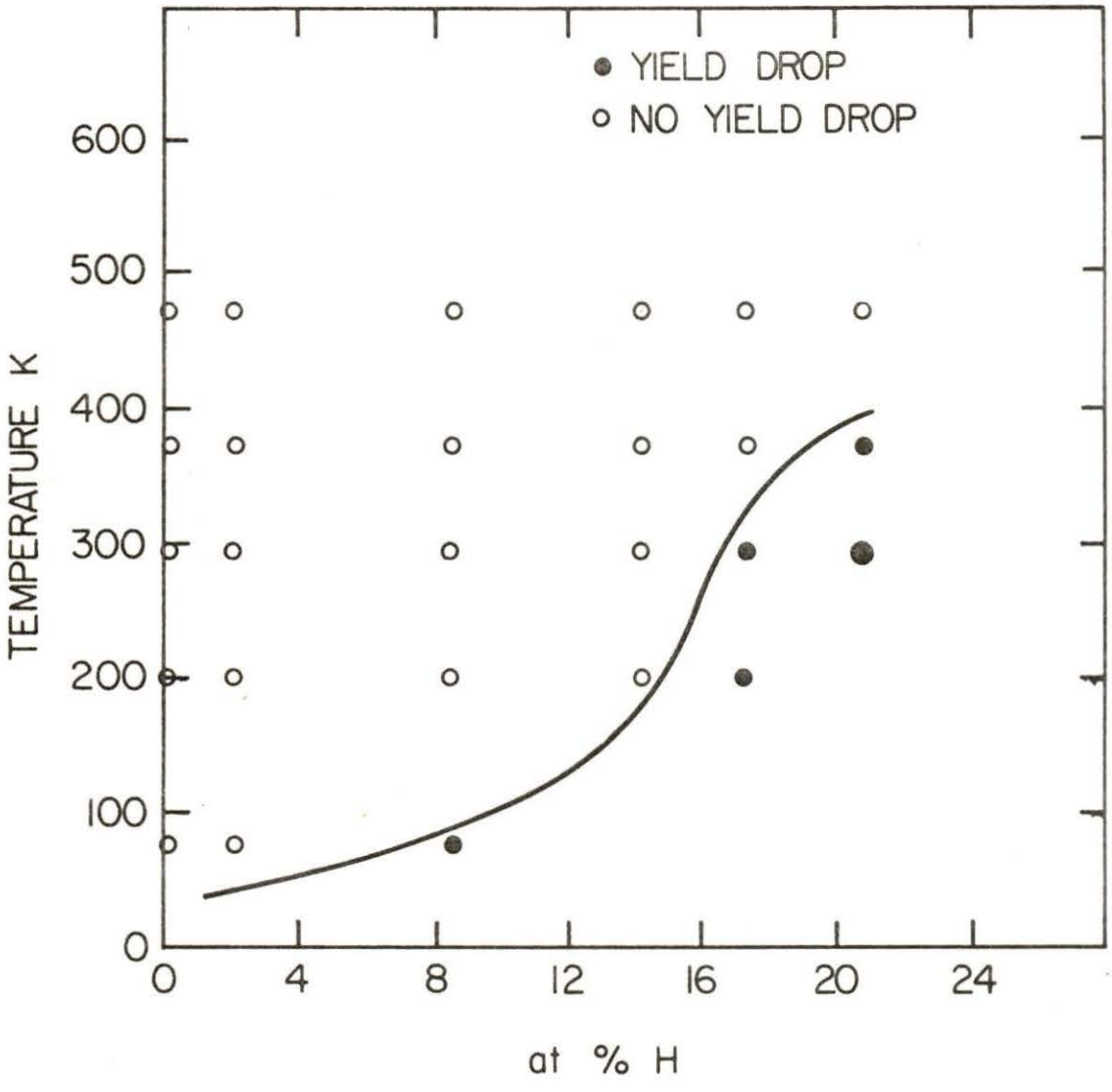

Fig. 6. Plot of the temperature concentration dependence of the onset of yield drops

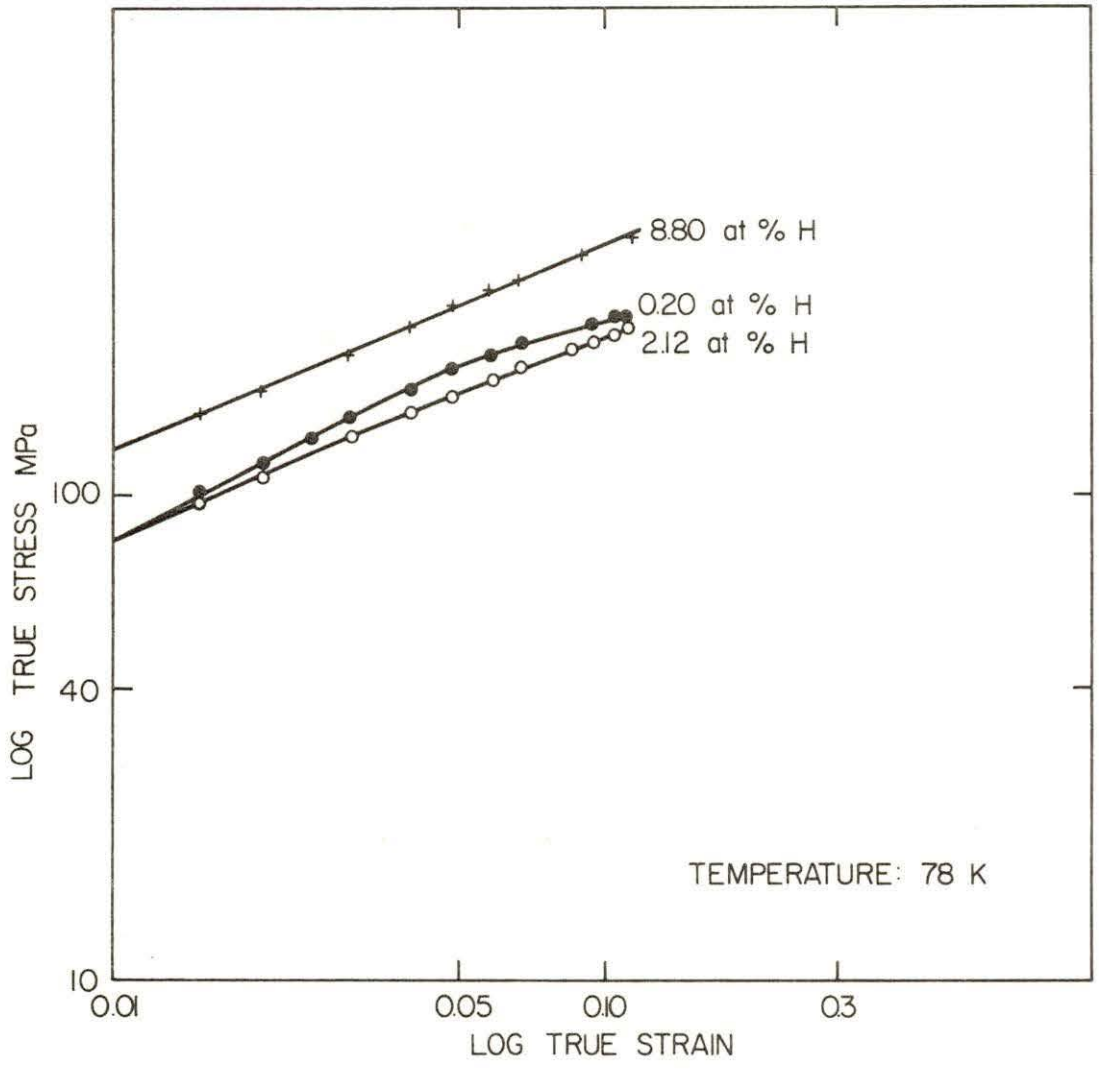

Fig. 7. Log true stress versus log true strain plots for scandium-hydrogen alloys tested at 78 K

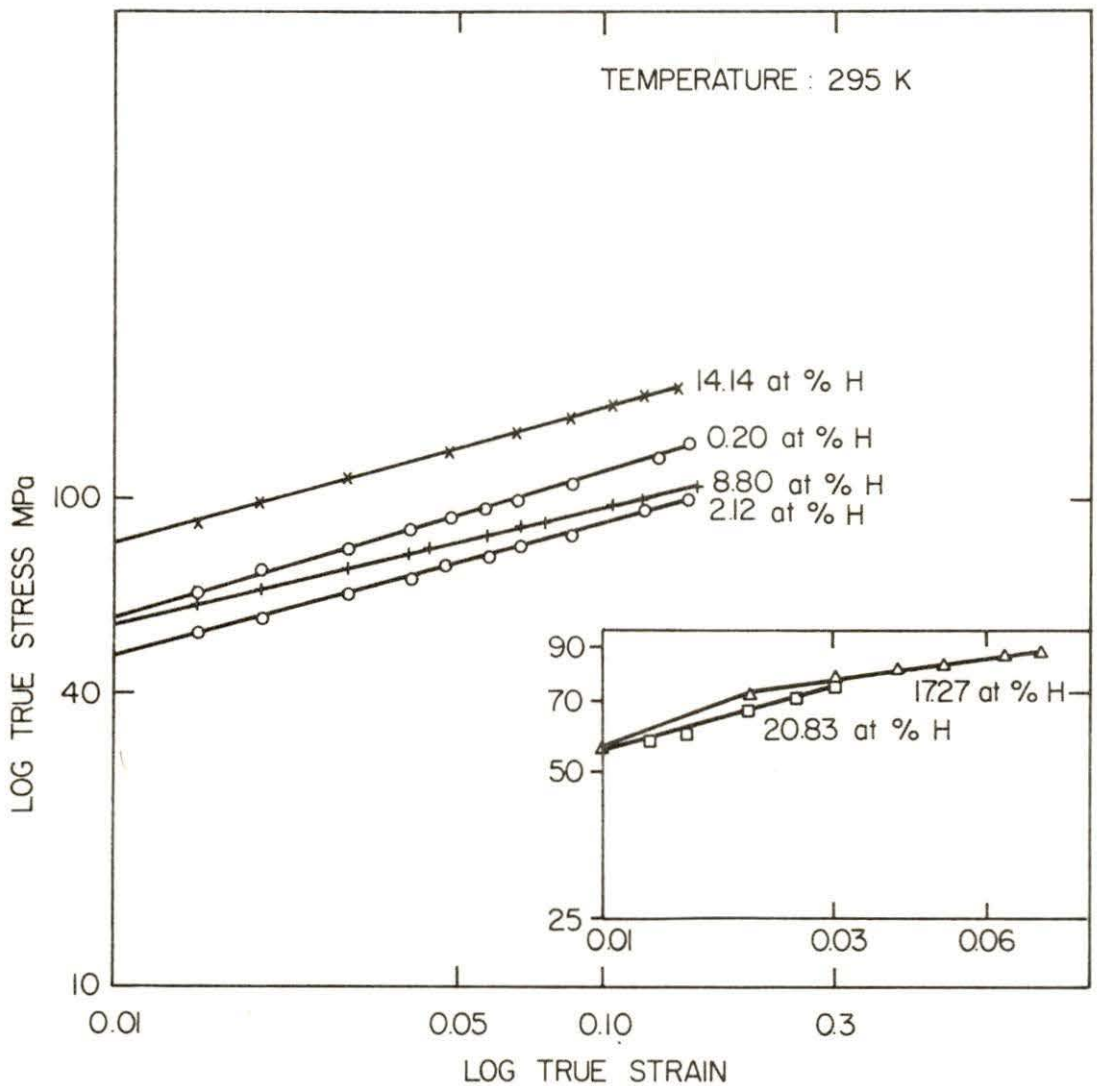

Fig. 8. Log true stress versus log true strain plots for scandium-hydrogen alloys tested at 295 K

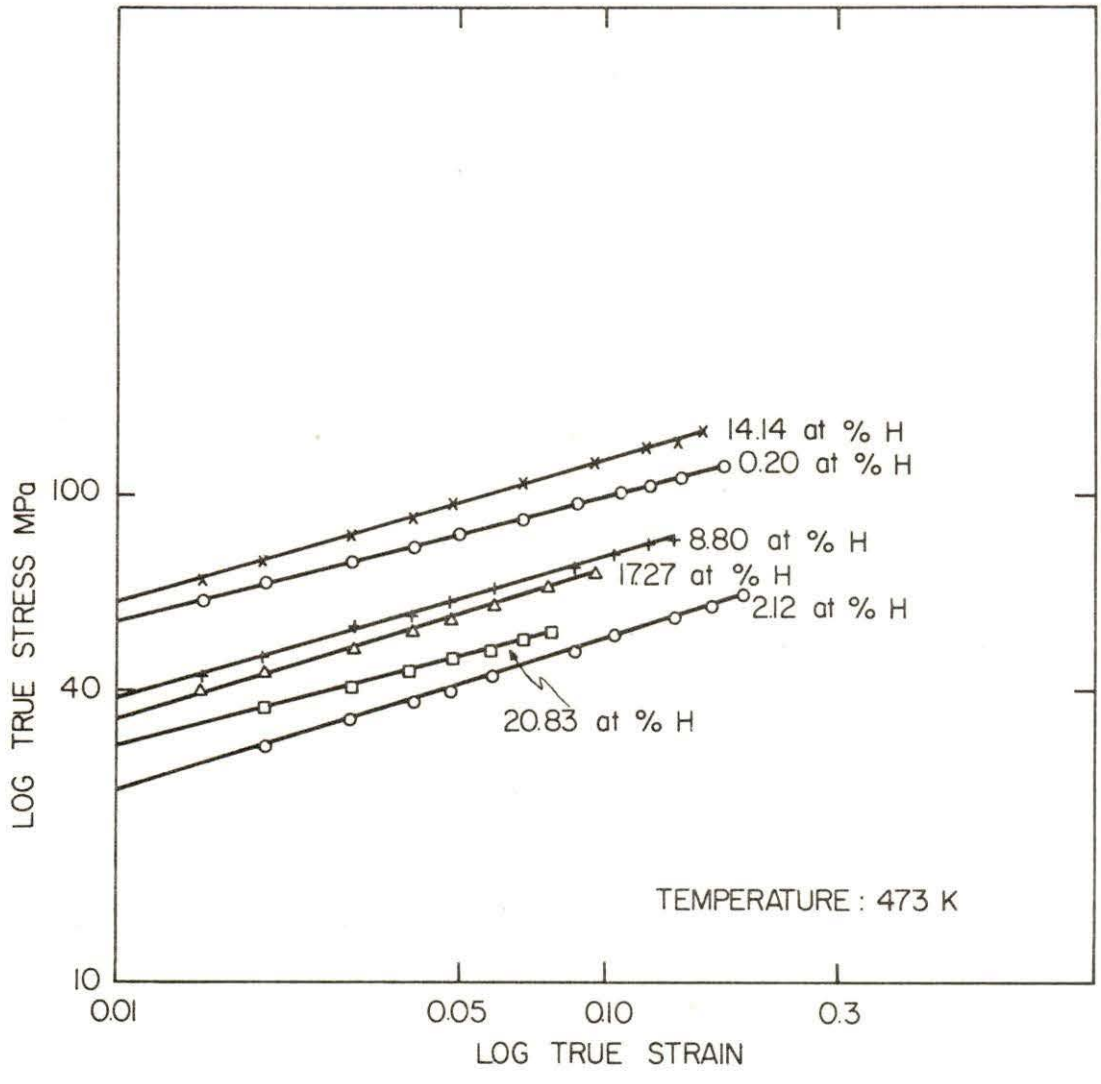

Fig. 9. Log true stress versus log true strain plots for scandium-hydrogen alloys tested at 473 K

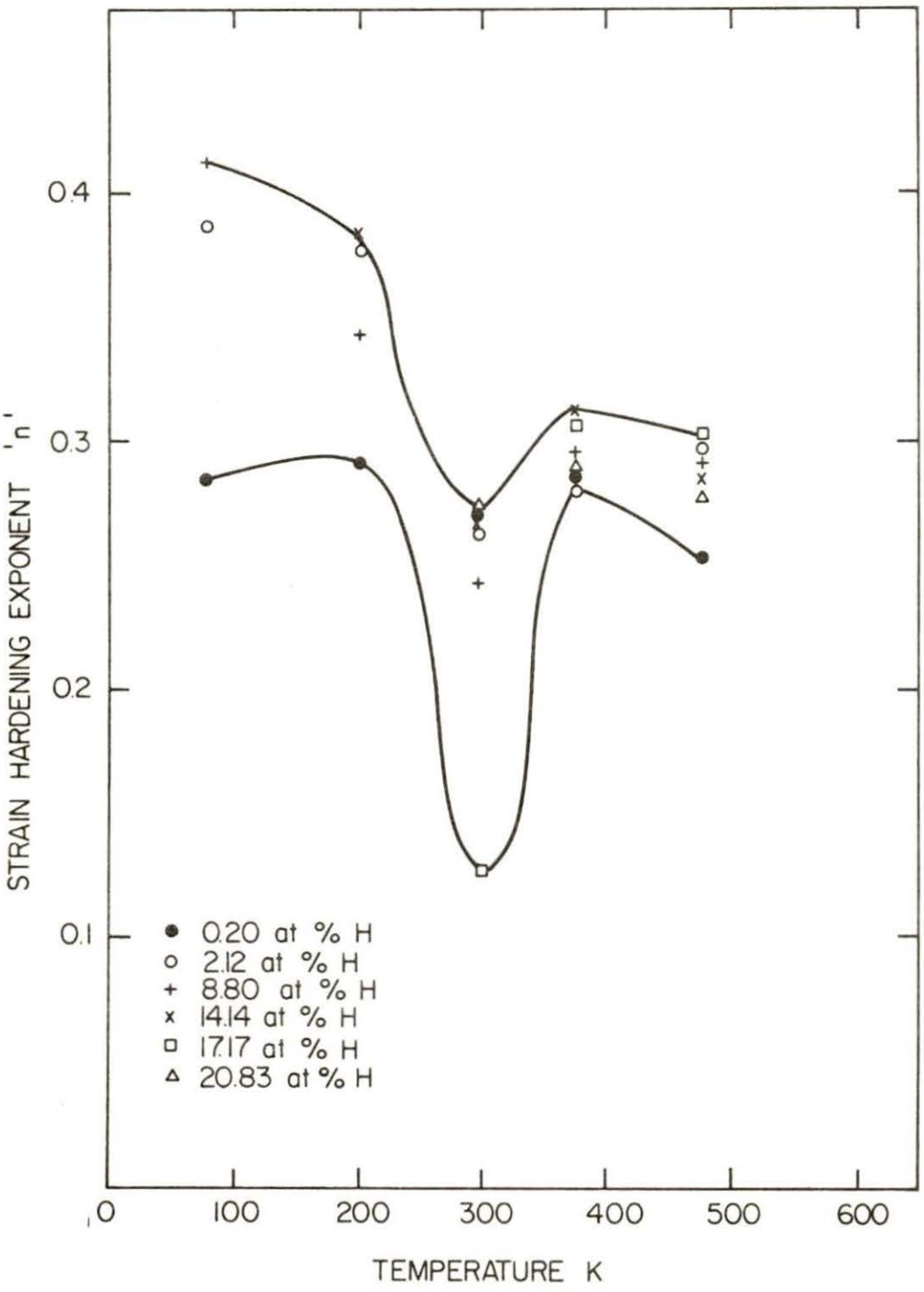

Fig. 10. Effect of temperature on the strain hardening exponent of scandium-hydrogen alloys

drop occurs between 200 K and 295 K. It is not clear that a significant decrease in strain hardening occurs in the pure scandium but, when hydrogen is added to the metal, the decrease is evident.

The ductility of scandium was found to be dependent on temperature and hydrogen content. Uniform elongation and reduction of area as a function of temperature are shown in Figs. 11 and 12 for all hydrogen concentrations employed. From the ductility-temperature curves it can be seen that, for the two lowest hydrogen bearing alloys, hydrogen did not lower the ductility. However, with the addition of 14.14 at% H and higher, scandium exhibits a ductile-to-brittle transition which is shifted to higher temperatures with increasing hydrogen content. These trends are demonstrated especially by the reduction of area in Fig. 12.

Fracture surfaces were examined by Scaning Electron Microscopy (SEM) and sectional specimens by optical microscopy. Fig. 13 shows SEM fractographs of samples containing 2.12, 8.80, 17.27, and 20.83 at% H which were tested at 295 K. It can be seen that the fracture mode changed from shear to cleavage. The fracture surface of scandium containing 2.12 at% H exhibited a limited number of voids characteristic of a ductile fracture. The fracture of scandium containing 20.83 at% H was planar and transgranular with a large number of transgranular cracks.

Examination of the internal section of unhydrogenated scandium revealed that voids were formed at all test temperatures, and that near the fracture surface the density of voids increased. However in the scandium-hydrogen alloys that were tested at temperatures above the ductile-to-brittle transition the number of voids decreased as function

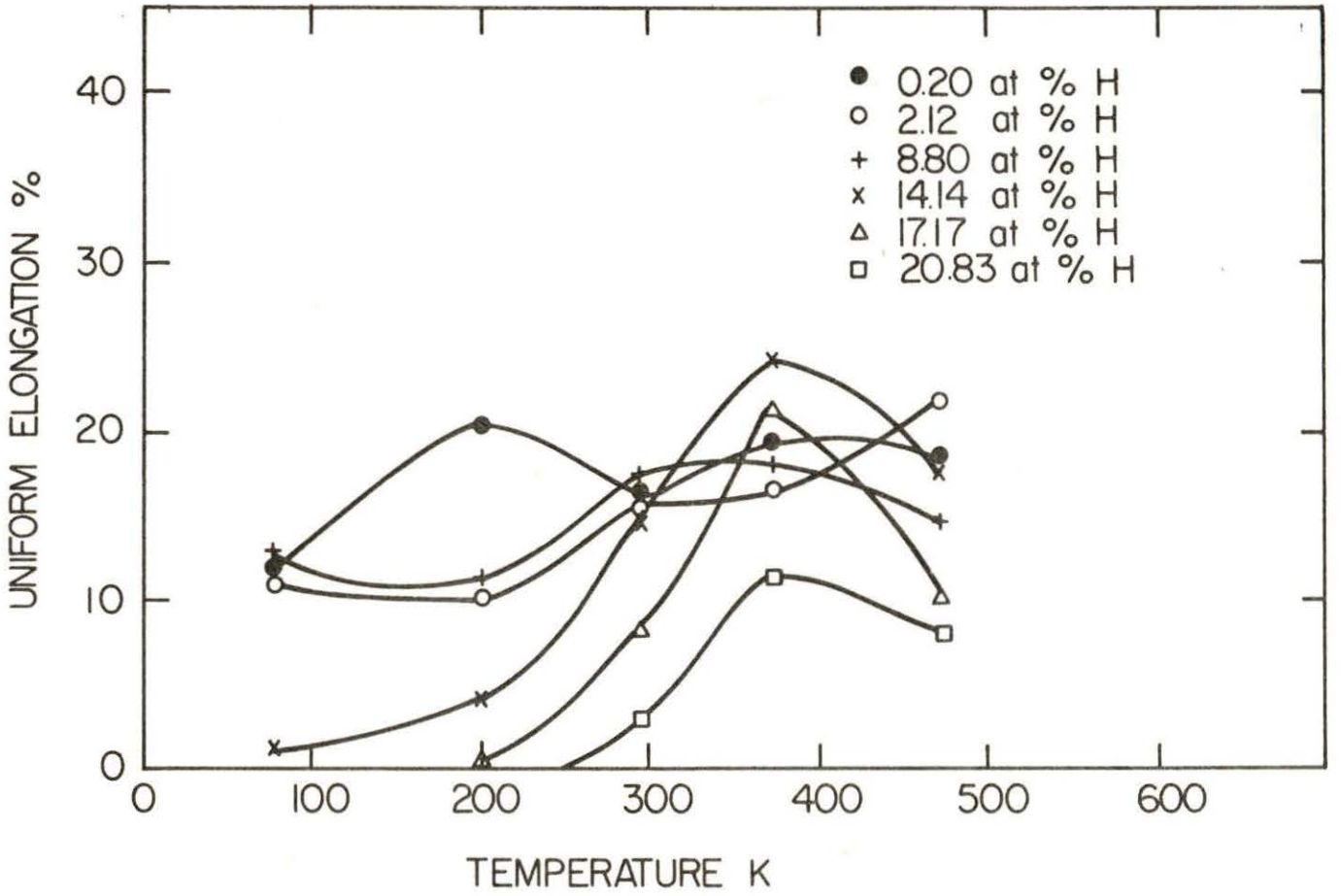

Fig. 11. Plot of uniform elongation versus temperature of scandium-hydrogen alloys

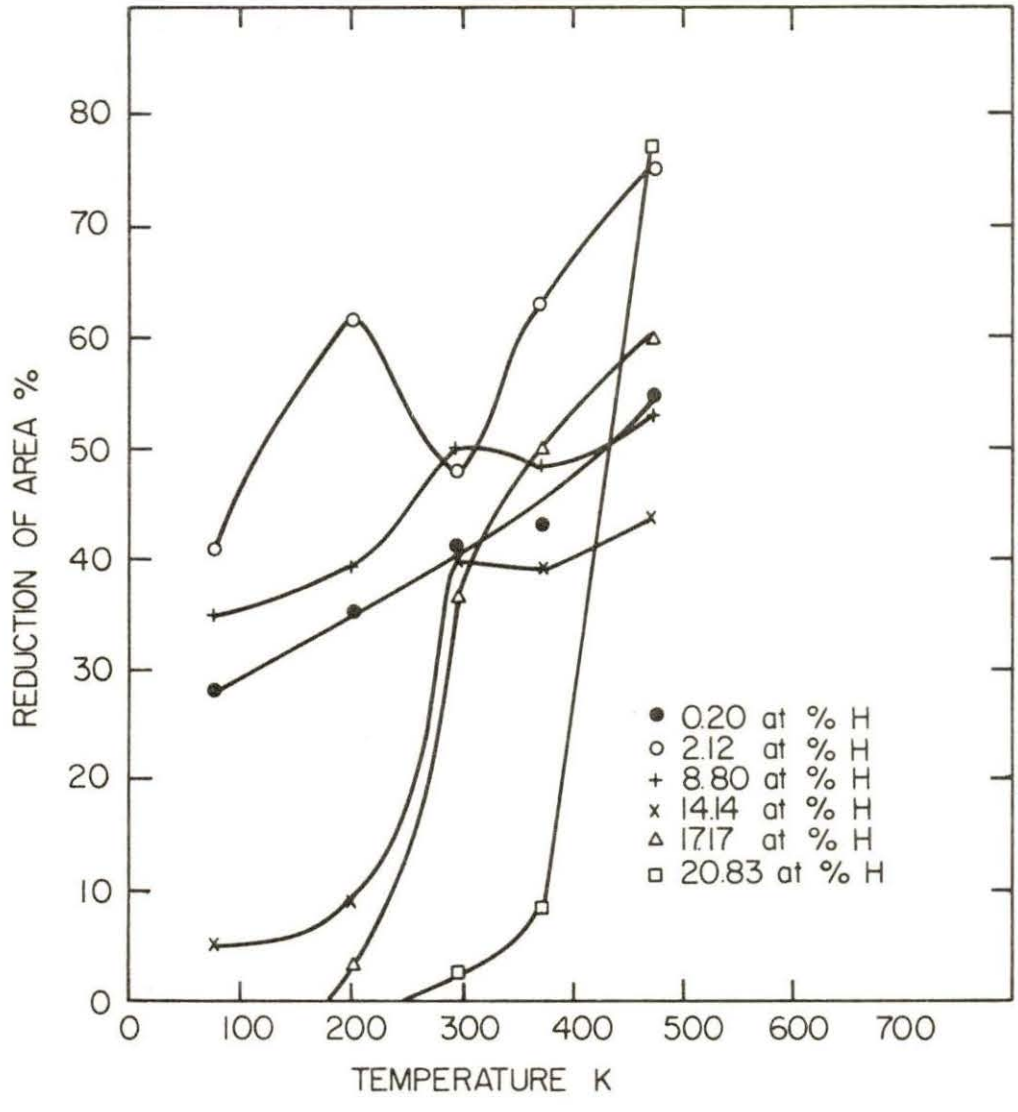

Fig. 12. Plot of reduction of area versus temperature of scandium-hydrogen alloys

Fig. 13. SEM fractographs of scandium containing 2.12, 8.80, 17.27, and 20.83 at % H and tested at 295 K. The fracture of scandium containing 2.12 at% H (a) was by shear, whereas the fracture of scandium containing 20.83 at% H (d) was by cleavage. Note the large number of cracks in (d)

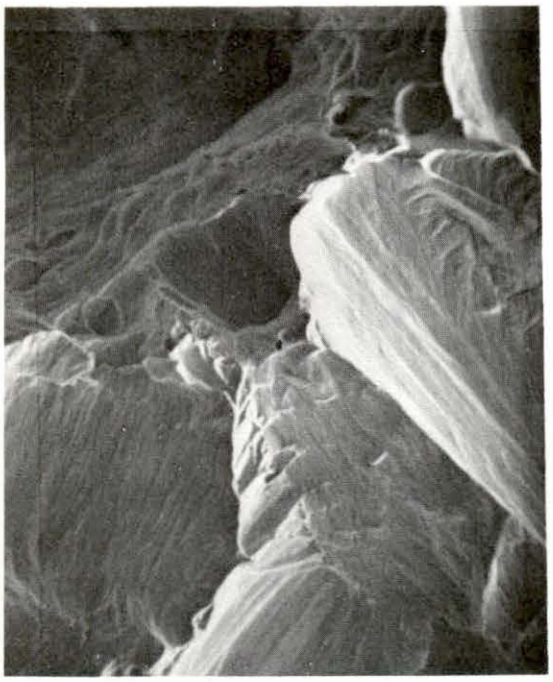

2.12 at% H (a) 240X

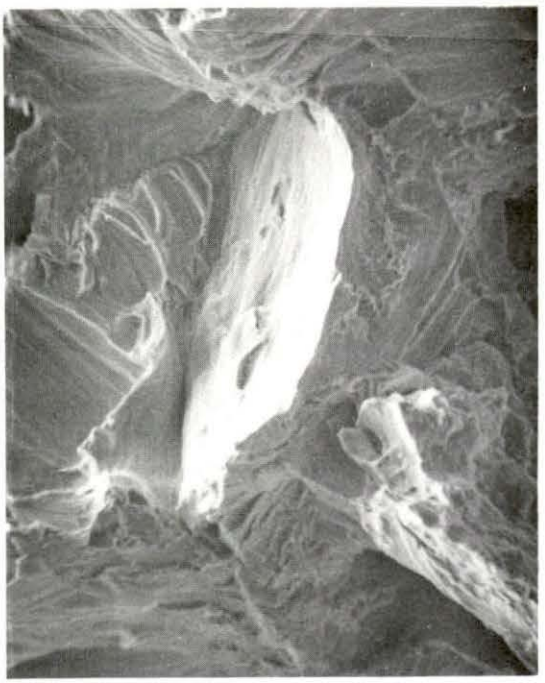

8.80 at% H (b) 250X

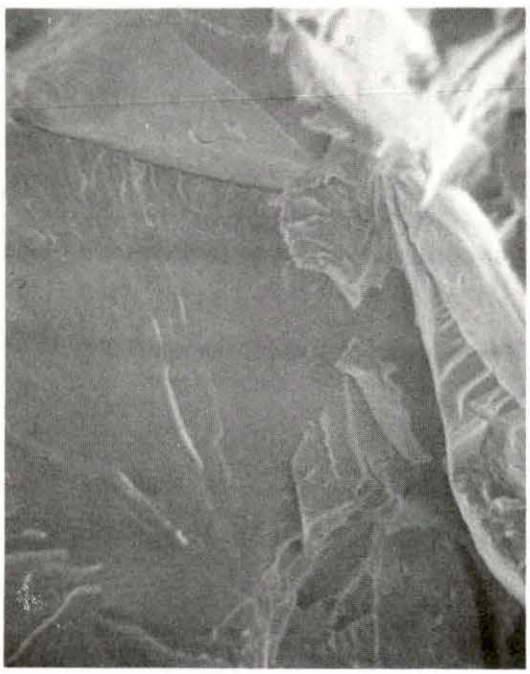

17.27 at% H (c) 225X

20.83 at% H (d) 225X

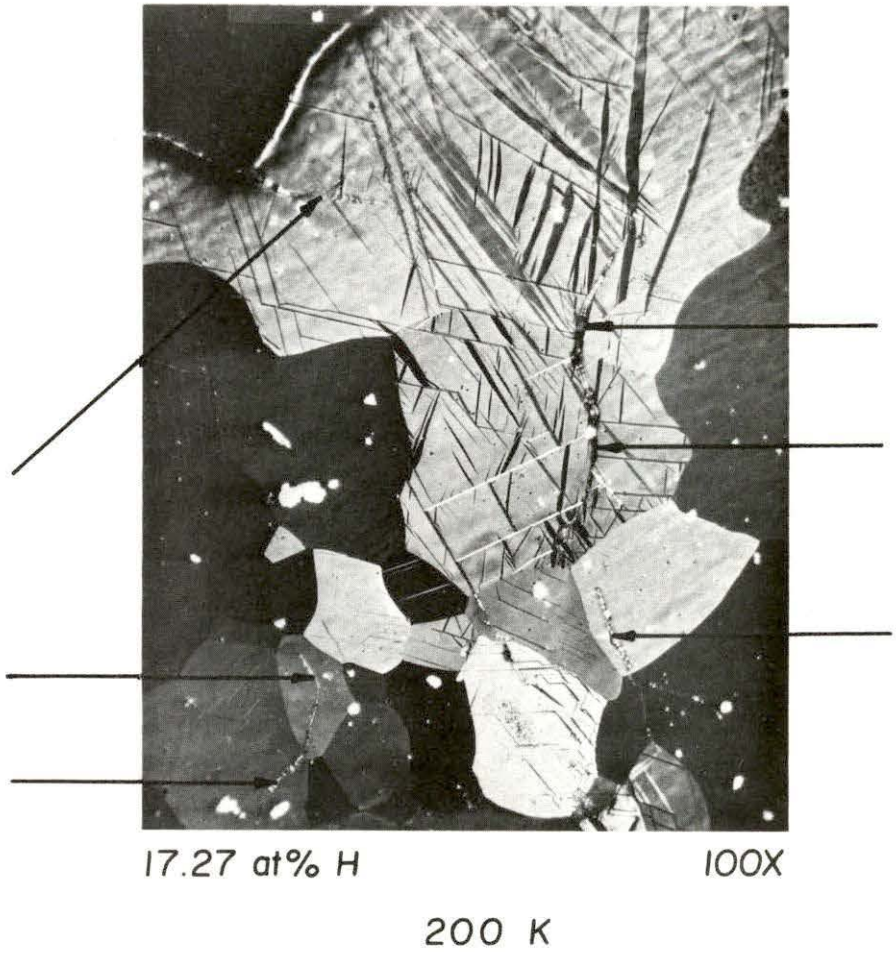

Fig. 14. Photomicrograph of scandium containing 17.27 at% H and tested at 200 K. The tensile axis is vertical and the arrows point to secondary cracks near the fracture surface. (As electropolished in 6% perchloric acid 94% methanol at 200 K, polarized light)

of increasing hydrogen content. In addition, scandium alloys which exhibited a ductile-to-brittle transition revealed cracks near the fracture surface as well as internal cracks when tested below the ductile-to-brittle transition. The cracks propagated transgranularly as shown in Fig 14.

Additional tensile tests were conducted on scandium containing 14.14 at% H at a strain rate of 3.33×10^{-2} sec^{-1} to assess the effect of strain rate on the ductile-to-brittle transition. From Fig. 15 where the reduction of area versus temperature of samples tested at strain rates of 3.33×10^{-5} sec^{-1} and 3.33×10^{-2} sec^{-1} is shown, it can be seen that the higher strain rate increased the ductile-to-brittle transition only by about 25 K.

Hydrogen in excess of the solid solubility limit in scandium revealed that the hydride phase was acicular in nature as shown in Fig. 16. Low temperature optical microscopy of the grip section of the hydrided tensile specimens revealed that no hydride precipitation occurred below 295 K. This observation corroborates the earlier results obtained by resistivity. From low temperature optical microscopy of the sample shown in Fig. 16, it was found that precipitation of additional hydrides did not occur, even after holding for four hours at 78 K.

The flow stress of scandium-hydrogen alloys containing 0.20, 2.12, 8.80, 14.14, and 20.83 at% H is plotted as a function of temperature in Figs. 17 through 21 respectively. Corresponding log flow stress versus temperature plots are shown in Figs. 22 through 26. The latter plots tend to divide the temperature dependence of the flow stress of hydrogen-

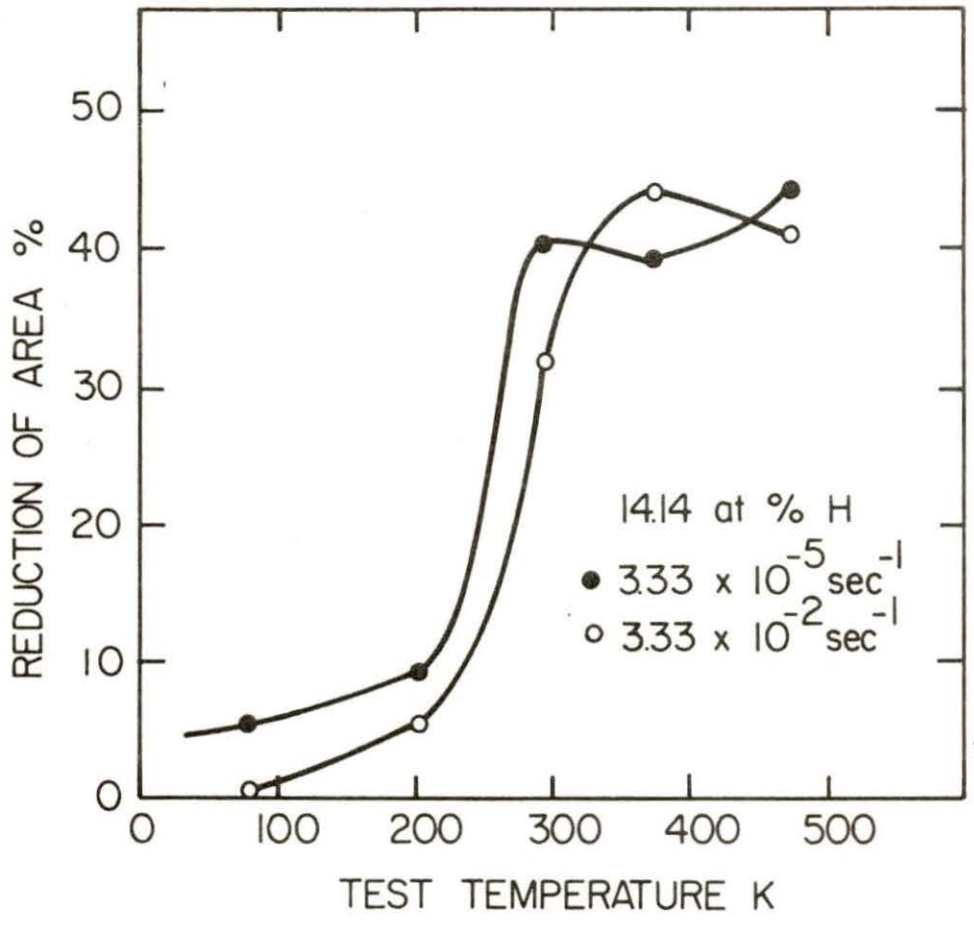

Fig. 15. The effect of increasing strain rate from 3.33×10^{-5} sec^{-1} to 3.33×10^{-2} sec^{-1} on the ductile-to-brittle transition of scandium containing 14.14 at% H

Fig. 16. Photomicrograph of scandium-hydride in scandium containing 34.60 at% H. (As electropolished in 6% perchloric acid 94% methanol at 200 K, oblique bright field)

charged scandium into three regions. The onset of the three regions is initially observed at 2.12 at% H and they are temperature and strain dependent as shown in Fig. 23. However at higher hydrogen concentrations, the three regions are no longer strain dependent and are best illustrated in Fig. 24, where the temperatures at which changes in slope occur are 175 K and 310 K. The most interesting feature of Figs. 22 through 26 is the change in slope of the second region, i.e. the region between 175 K and 310 K, as the hydrogen content is increased. The hydrogen induced changes in the flow stress behavior of scandium is associated with low temperature strengthening. A comparison of low temperature stress values at a given strain indicate that scandium is solution strengthened when the hydrogen content is above 2.12 at% . In addition the rapid decline in log flow stress between 175 K and 310 K correlates with the decrease in strain-hardening exponent in Fig. 10.

From Fig. 27 where the yield strength versus temperature is plotted for all hydrogen levels, it can be seen that, at 78 K, scandium is slightly solution softened by 2.12 at% H, whereas the addition of 8.80 at% H and 14.14 at% H cause substantial solution strengthening. If the 17.27 and 20.83 at% H curves are extrapolated to 78 K they also show solution strengthening, but not to the extent exhibited by the 14.14 at% hydrogen alloy. In other words, solution strengthening appears to peak near 14.14 at% H. As the test temperature is increased there is a steep drop in yield strength up to 300 K. Above 300 K the yield strength continues to decrease as a function of increasing temperature but at a smaller

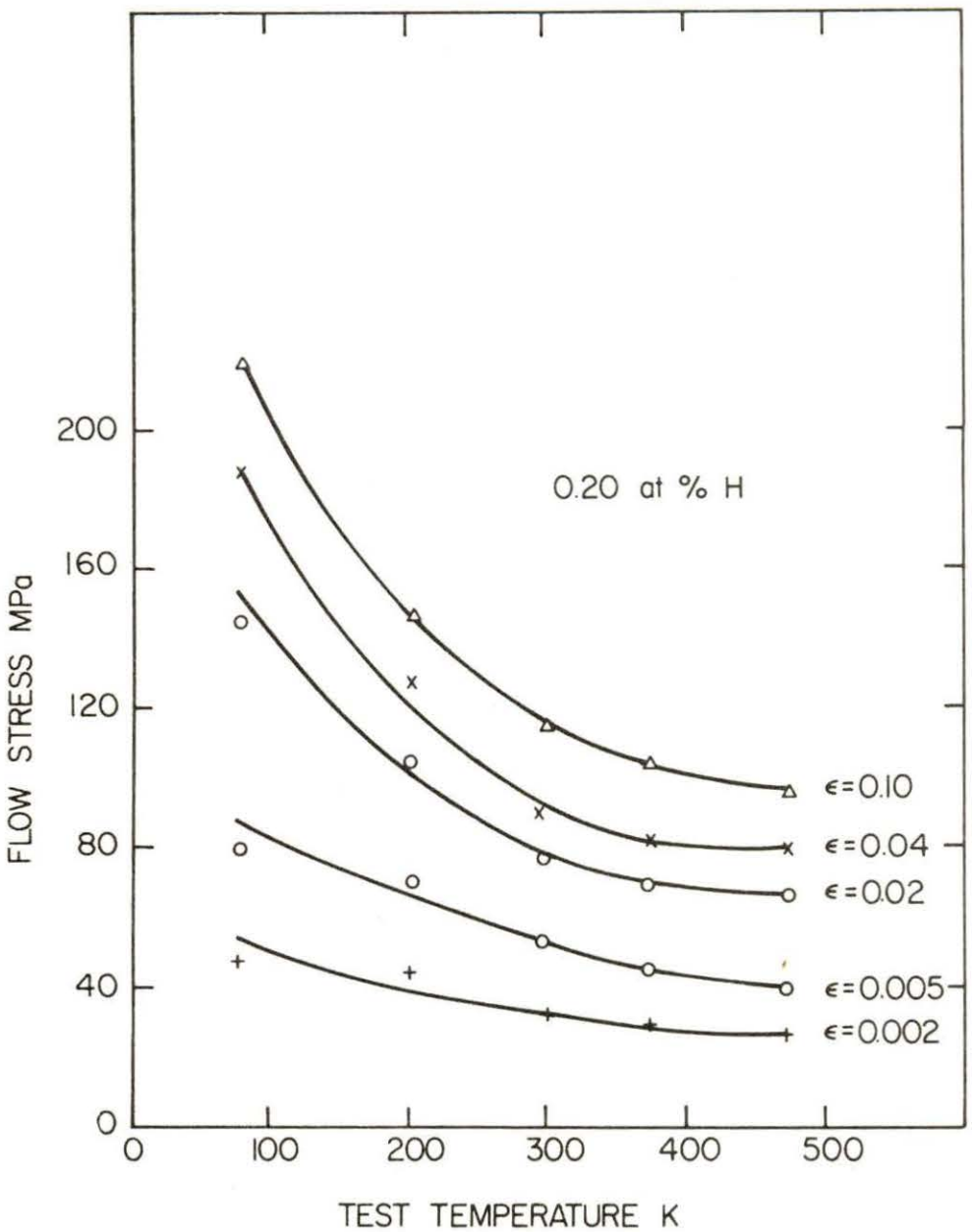

Fig. 17. Flow stress versus temperature for scandium containing 0.20 at% H for various strains

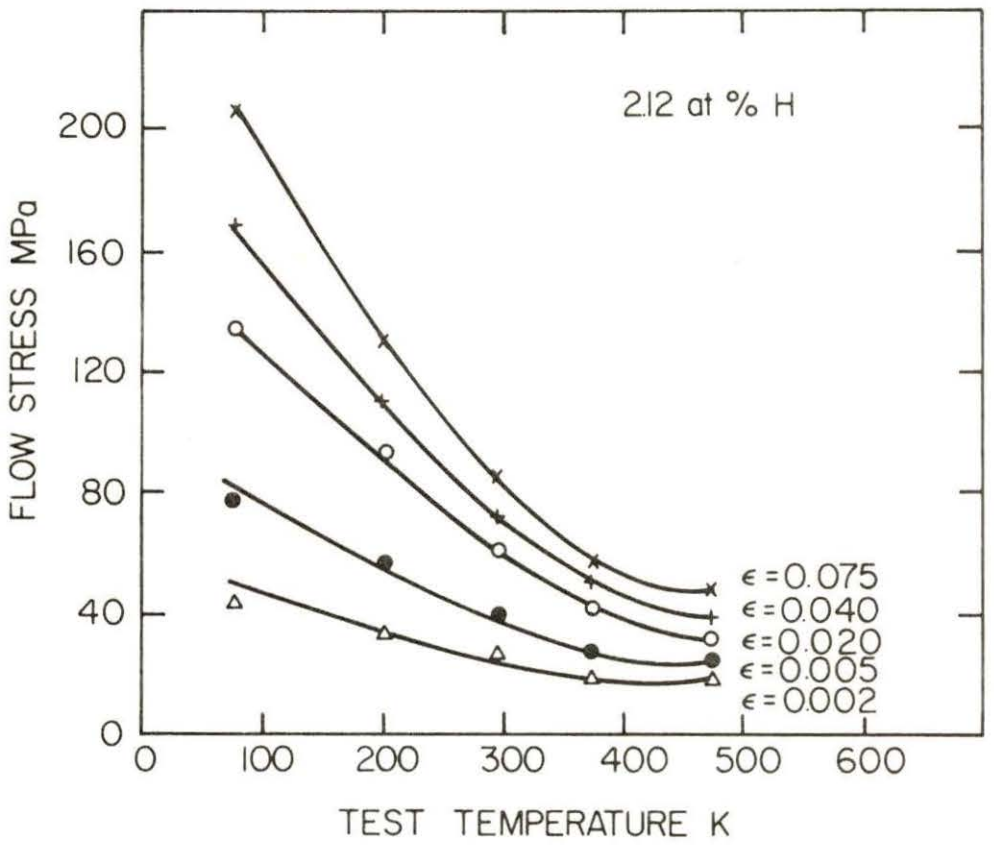

Fig. 18. Flow stress versus temperature for scandium containing 2.12 at% H for various strains

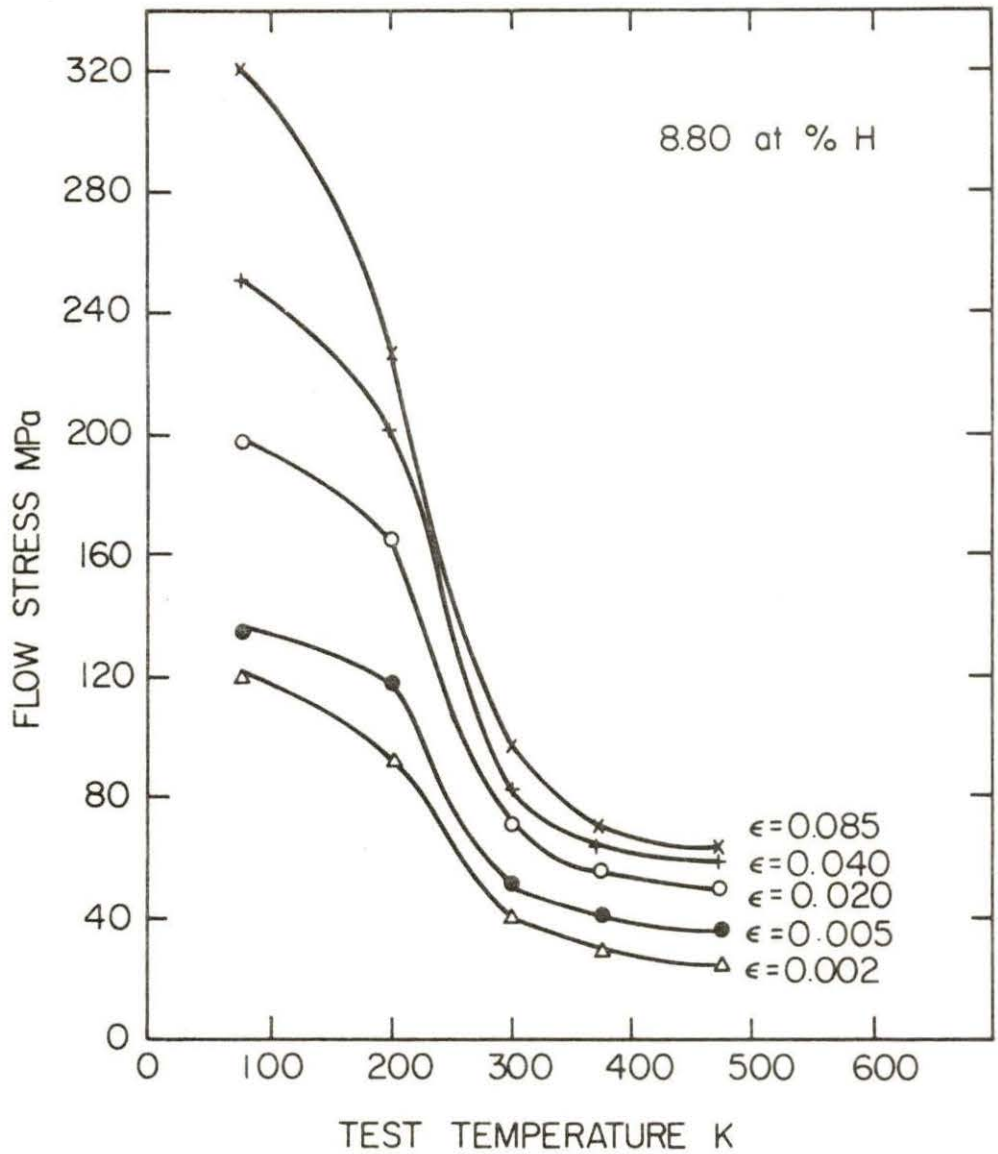

Fig. 19. Flow stress versus temperature for scandium containing 8.80 at% H for various strains

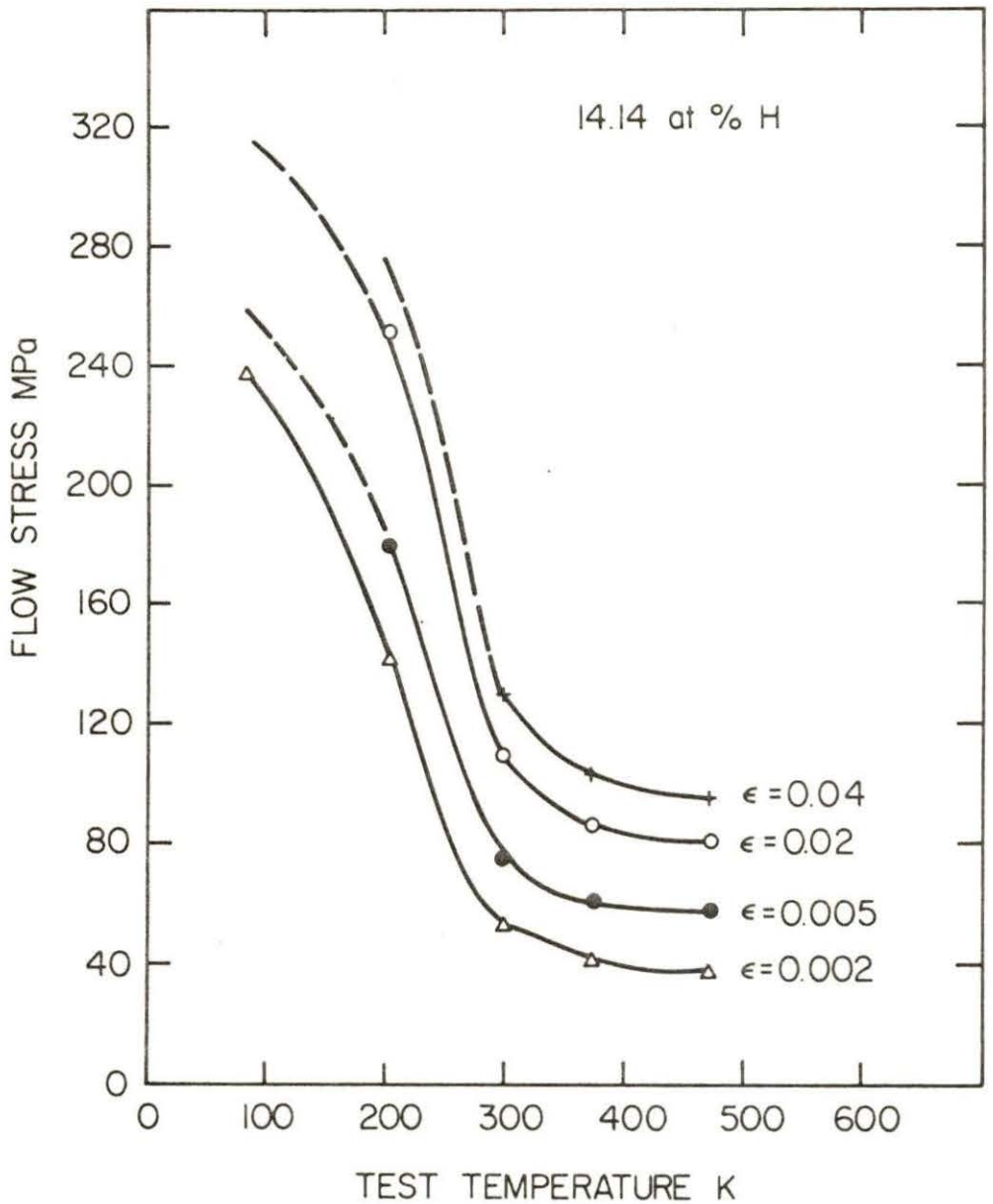

Fig. 20. Flow stress versus temperature of scandium containing 14.14 at% H for various strains

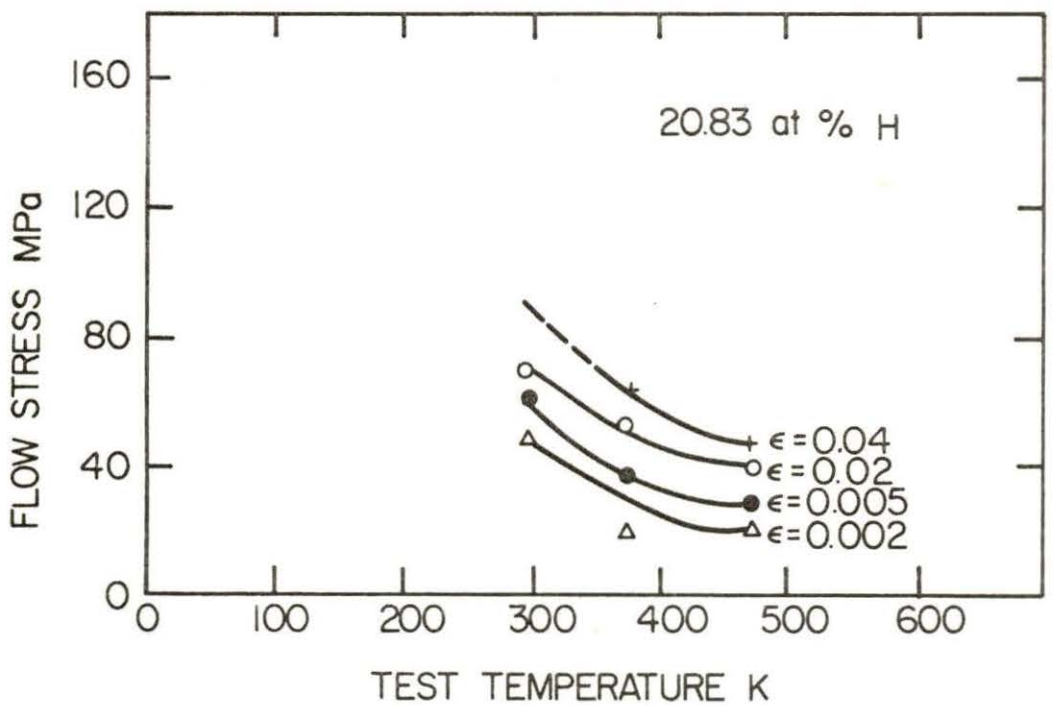

Fig. 21. Flow stress versus temperature of scandium containing 20.83 at% H for various strains

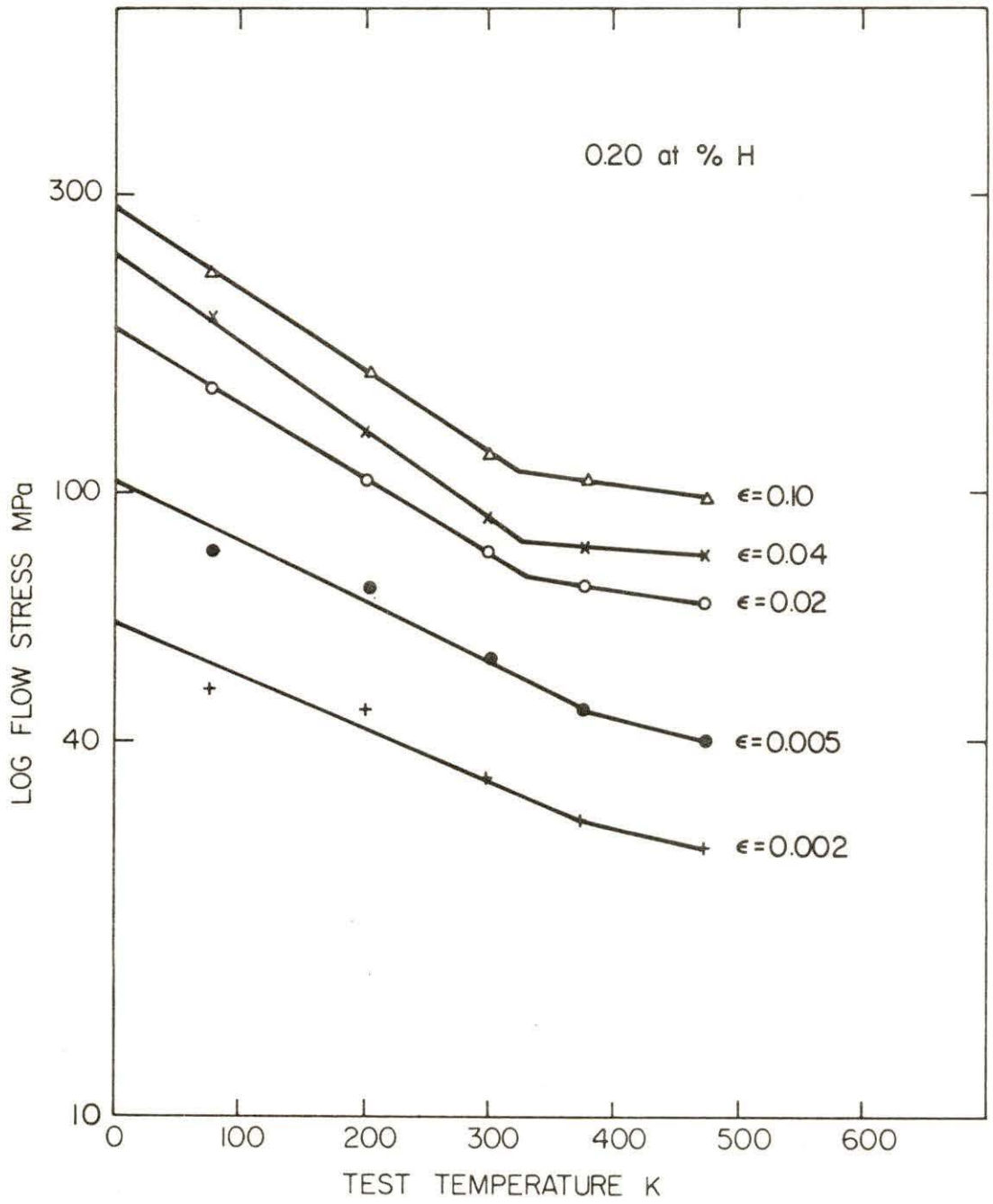

Fig. 22. Log flow stress versus temperature of scandium containing 0.20 at% H for various strains

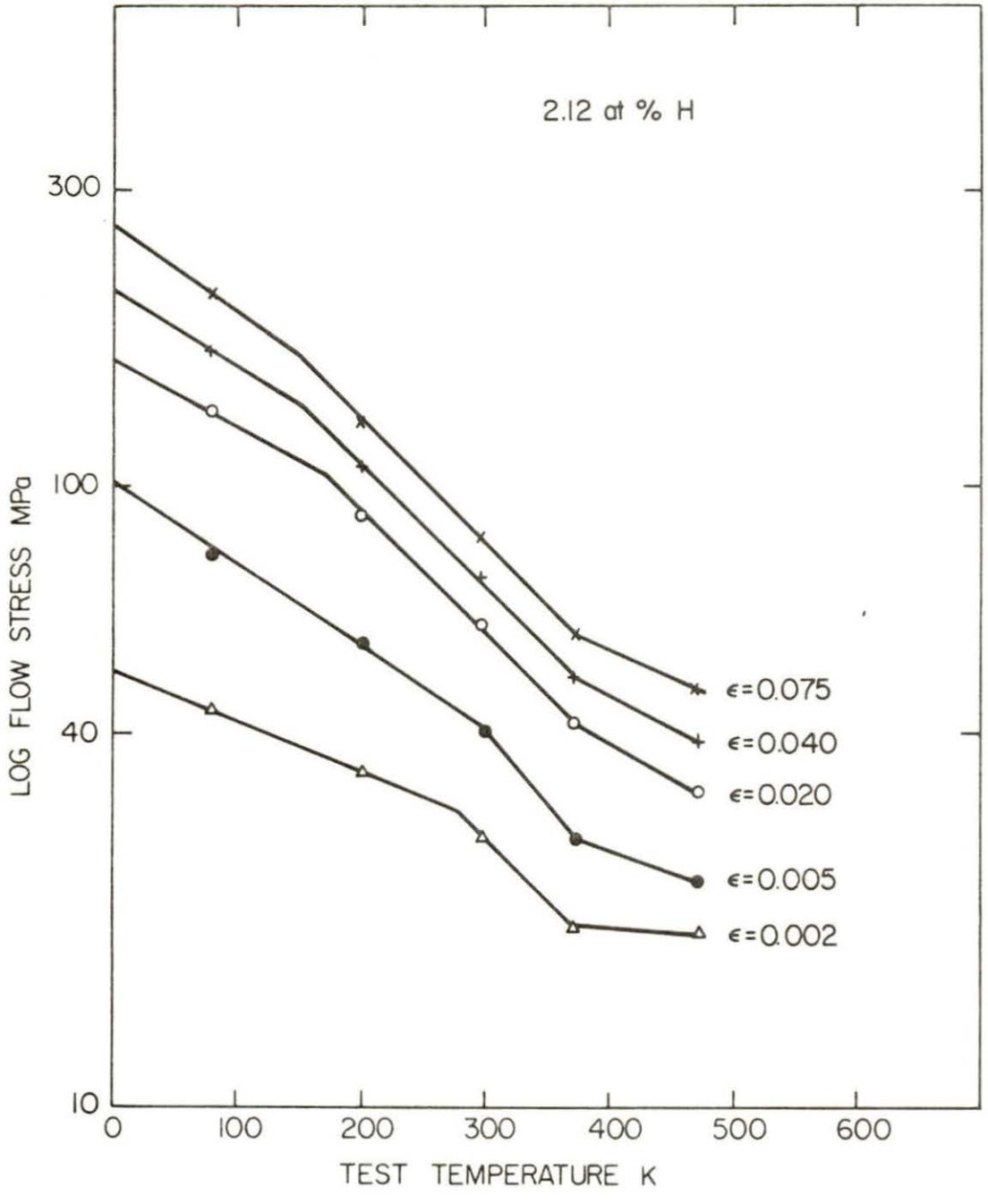

Fig. 23. Log flow stress versus temperature of scandium containing 2.12 at% H for various strains

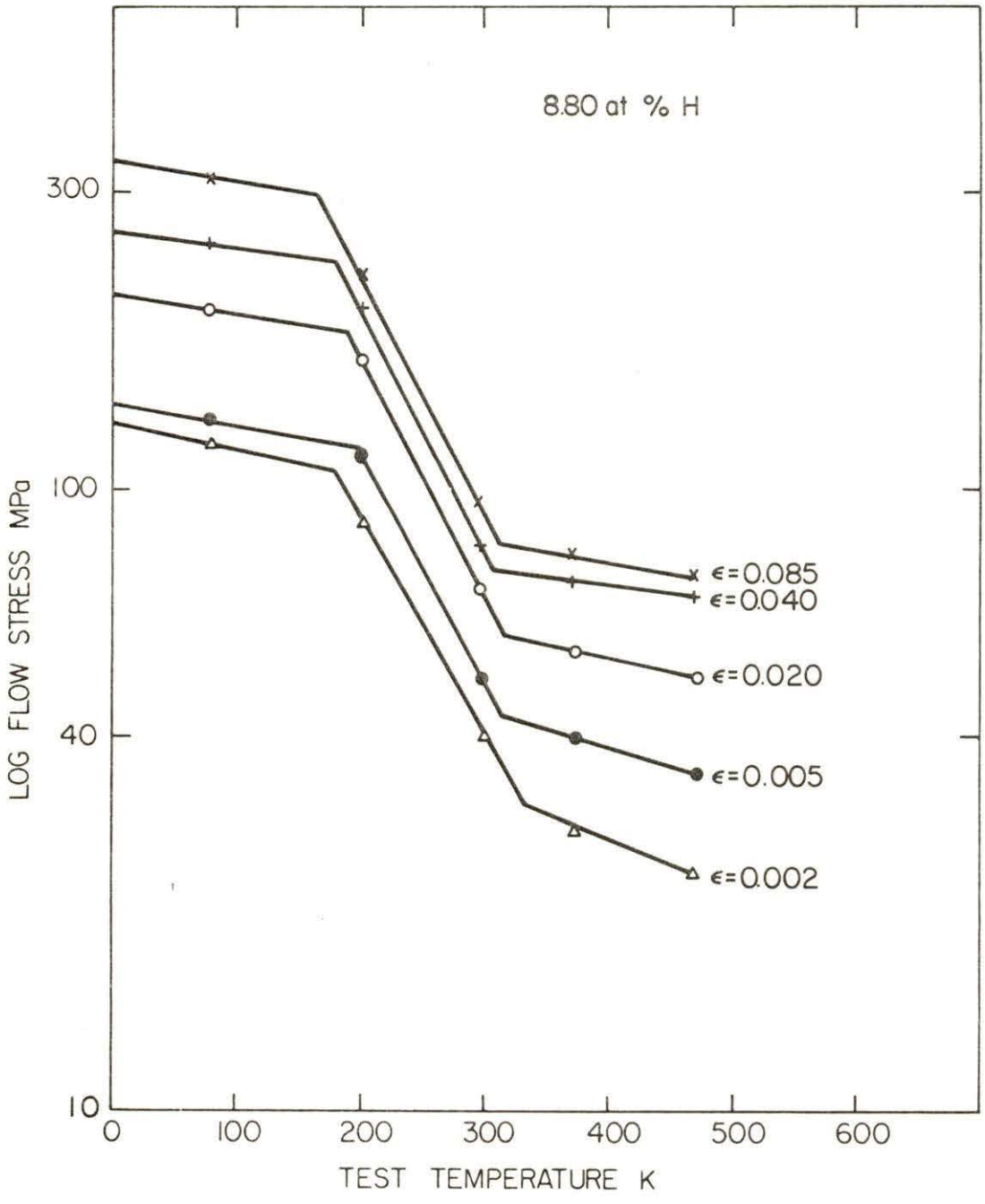

Fig. 24. Log flow stress versus temperature of scandium containing 8.80 at% H for various strains

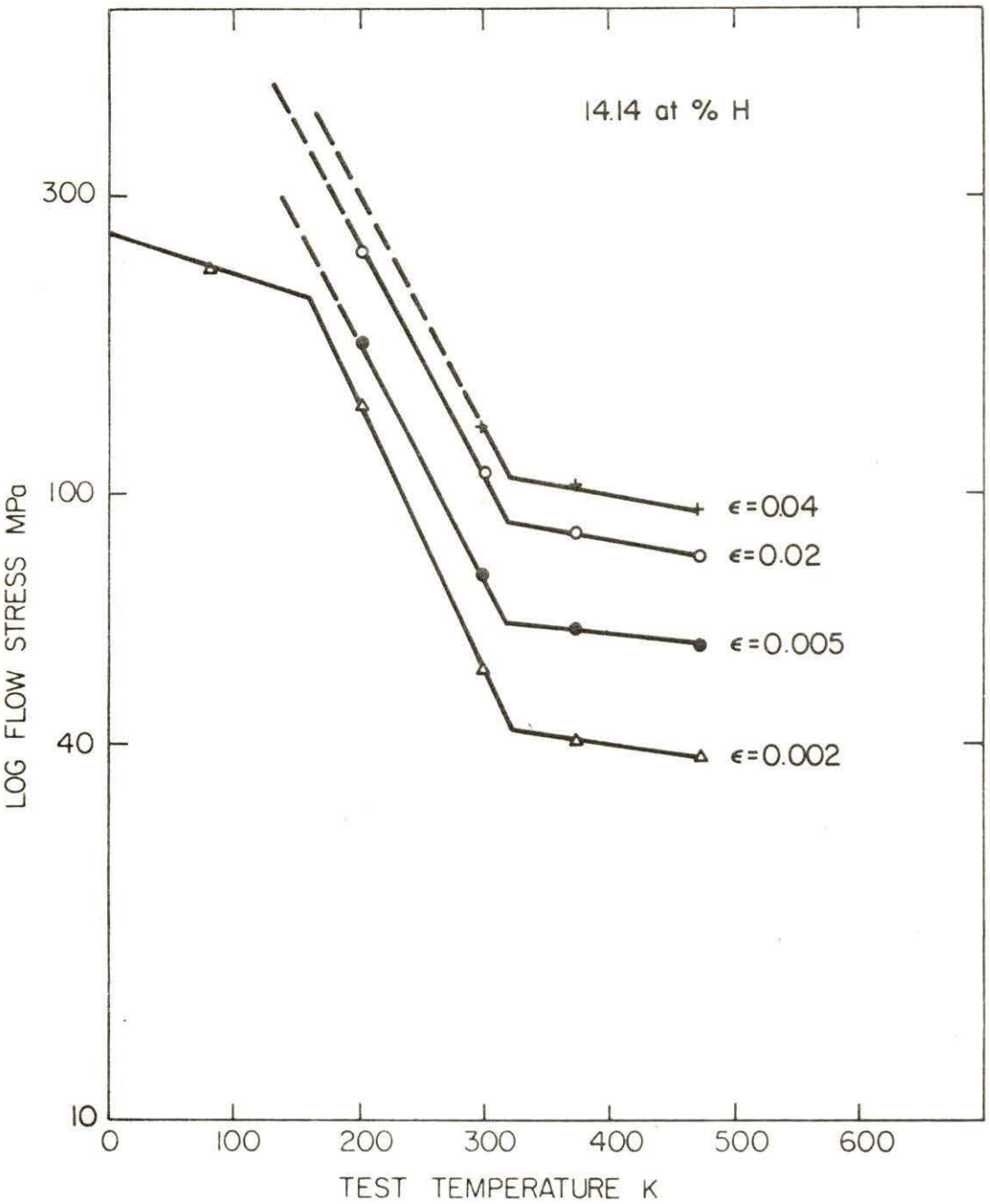

Fig. 25. Log flow stress versus temperature of scandium containing 14.14 at% H for various strains

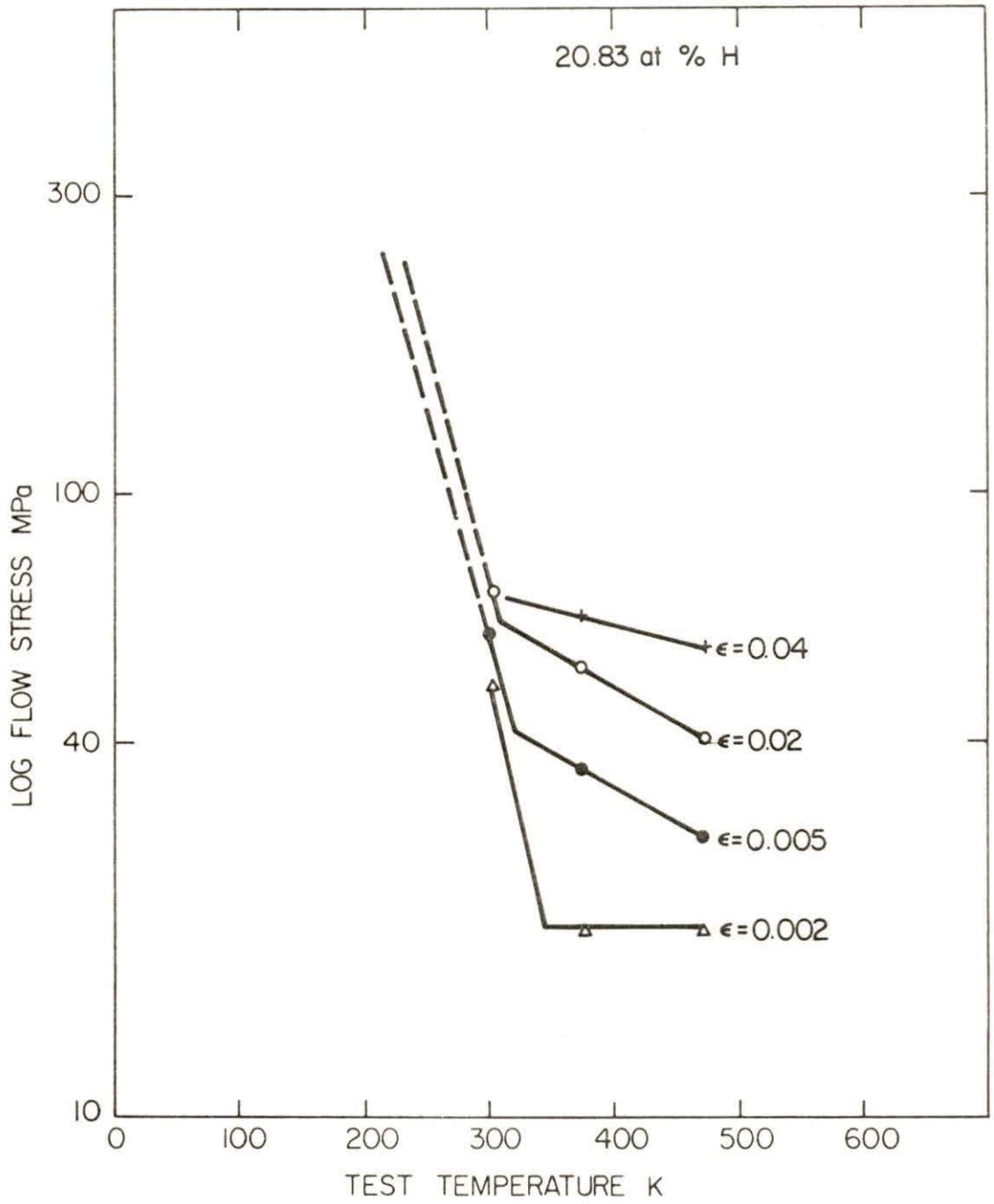

Fig. 26. Log flow stress versus temperature of scandium containing 20.83 at% H for various strains

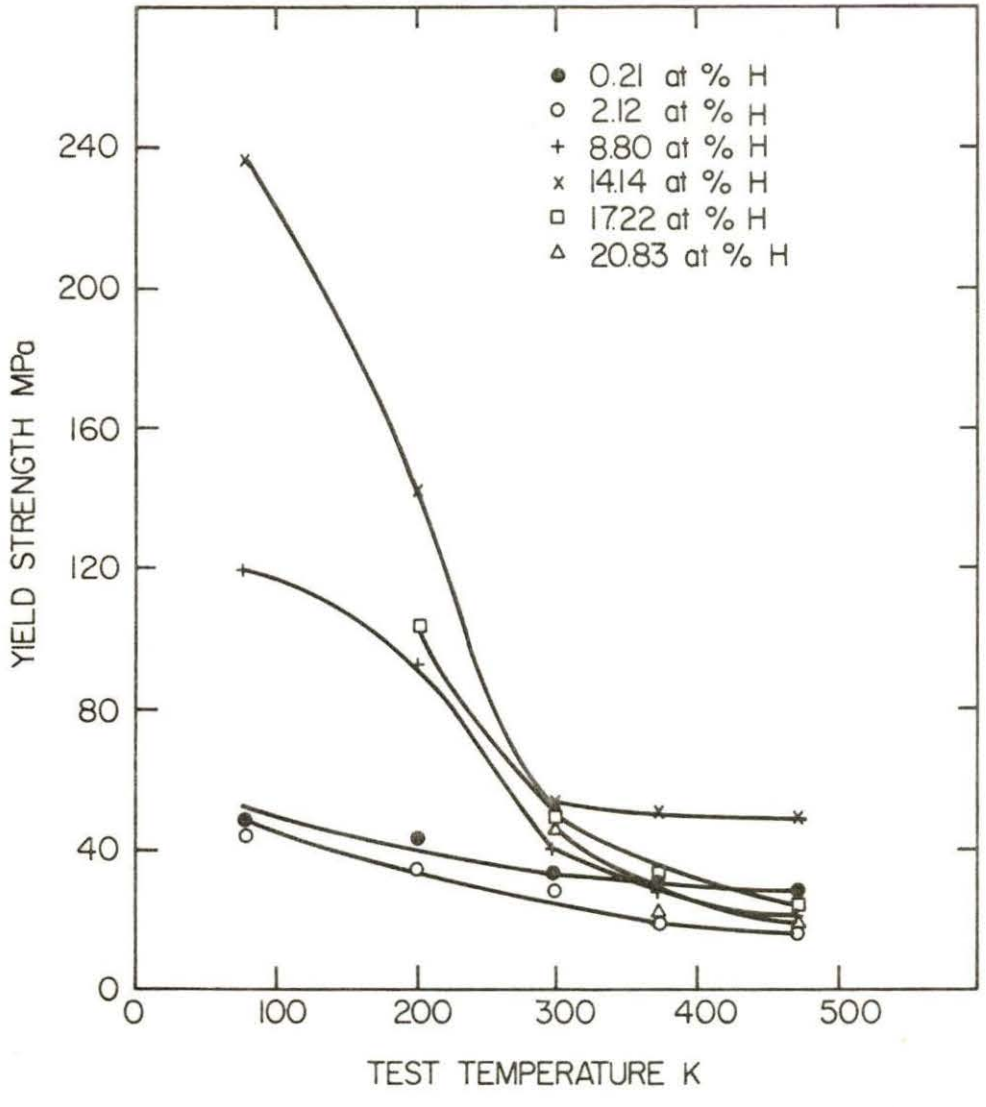

Fig. 27. Plot of yield strength versus temperature for all scandium-hydrogen alloys

rate compared to the temperature range of 78 K and 300 K. In fact, strengthening due to hydrogen in solid solution diminishes at 373 K, and at 473 K the yield strength of all scandium-hydrogen alloys, except for 14.14 at% H, was lower than pure scandium. The yield strength of scandium containing 14.14 at% H appears to reach a plateau region at test temperatures greater than 295 K.

The variation of the strain rate sensitivity and pseudo-activation volume as a function of strain for scandium containing 14.14 at% H are shown in Figs. 28 and 29. In this investigation a pseudo-activation volume is used because the Taylor factor (M) or orientation factor used for converting true tensile stress to shear stress is not known for scandium. The strain rate sensitivity was found to peak at 295 K and to be strain dependent. The pseudo-activation volume was found to be strain independent from 200 K to 373 K, however at 473 K it decreased as function of increasing temperature.

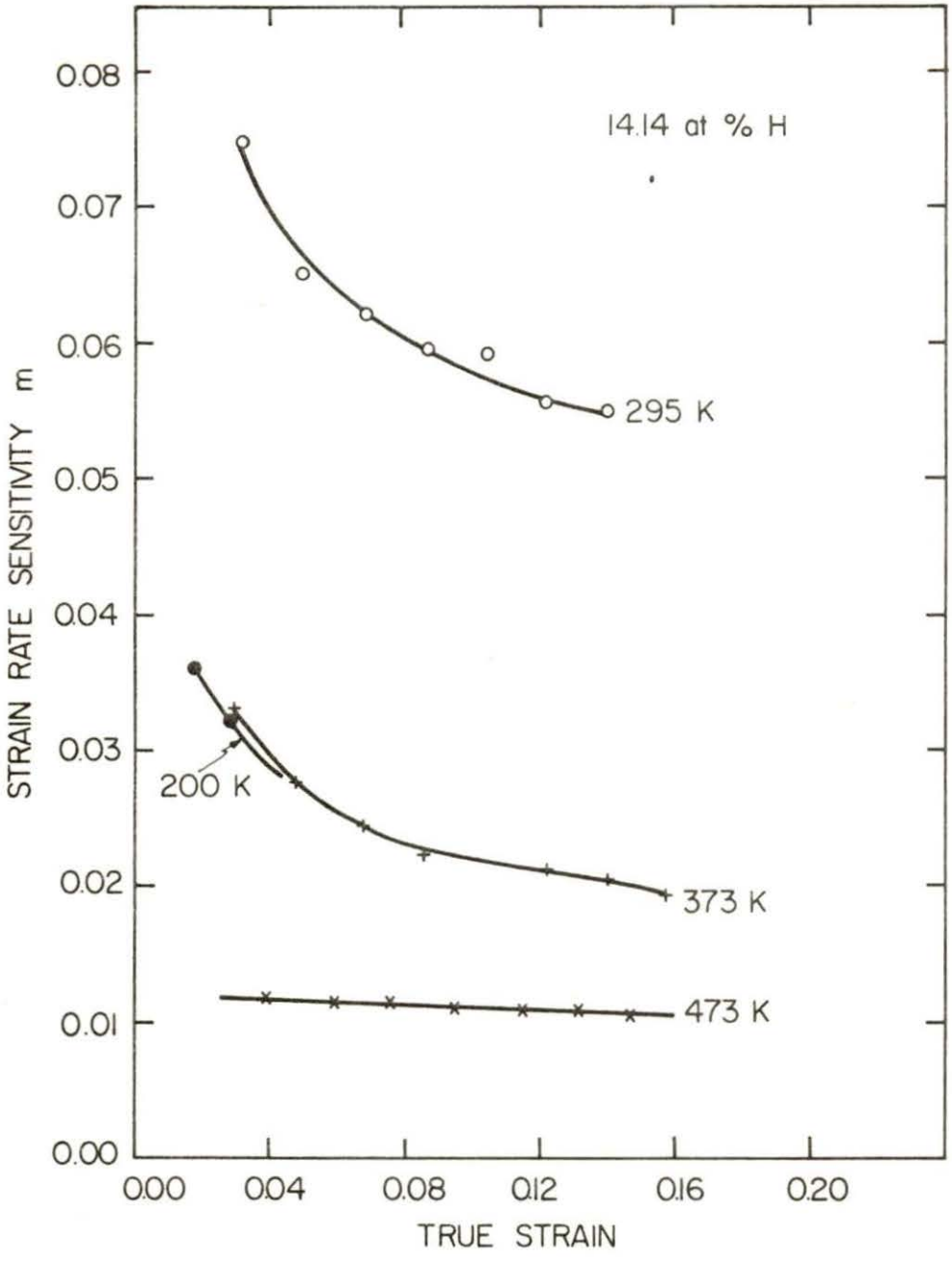

Fig. 28. Plot of strain rate sensitivity versus true strain for scandium containing 14.14 at% H at various temperatures

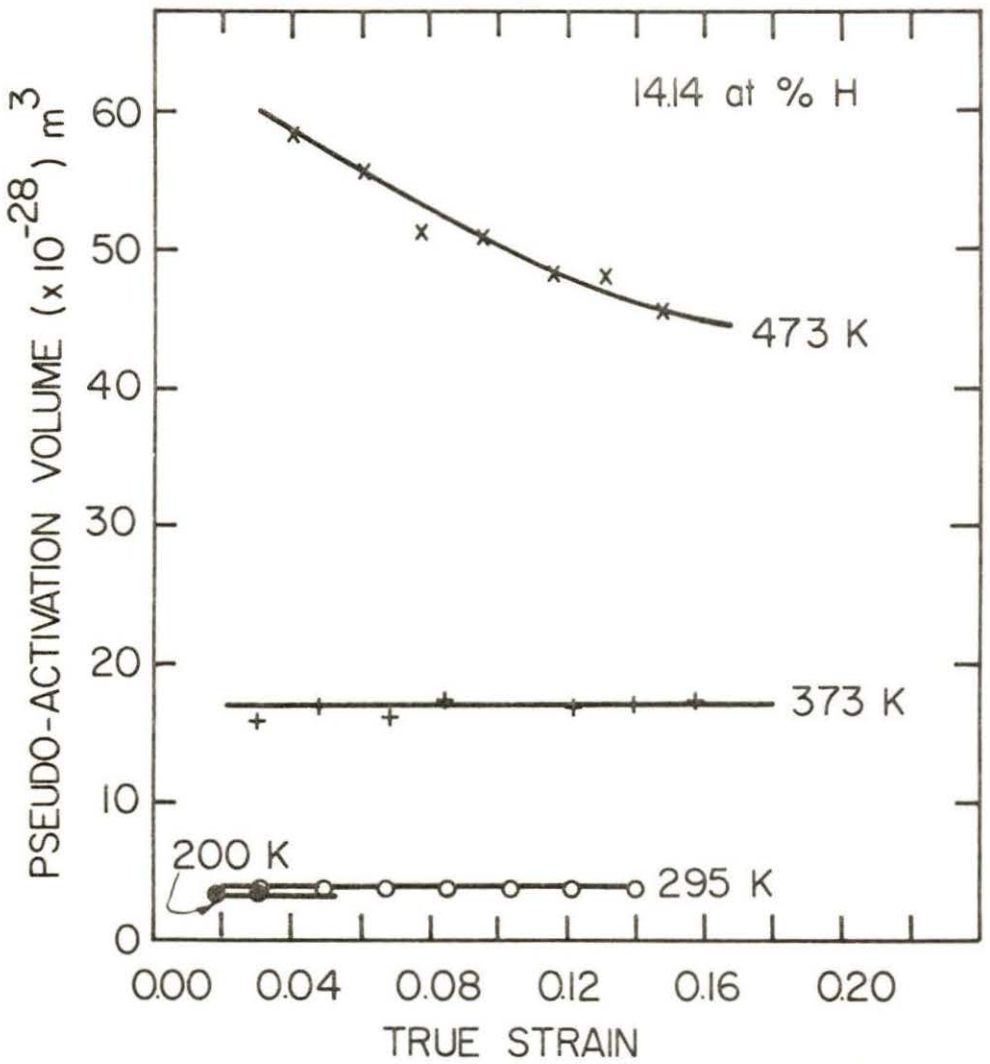

Fig. 29. Plot of pseudo-activation volume versus strain for scandium containing 14.14 at% H at various temperatures

DISCUSSION

The detrimental effects of hydrogen in solid solution or in the form of a precipitated hydride phase on the mechanical properties of metals, especially on plastic strain to failure and toughness, is an area of primary importance. It is an accepted fact, that in hydride forming systems, the hydride phase has a much lower ductility than the pure metal matrix and thus, the loss in ductility has been usually attributed to the presence of a brittle hydride phase which precipitated from solid solution upon cooling or was stress induced. While there is no doubt that the hydride phase will fracture at lower strains (stresses) than the matrix, any fracture model must include the fracture of the matrix rather than the hydride. A fracture process entirely dependent on the hydride phase can only be envisioned if massive hydrides are present throughout the metal matrix, thus providing a continous path for the propagation of cracks.

Sherman et al. (30) have addressed themselves to the critical question as to whether the precipitation of the hydride phase was the controlling step in the embrittlement of vanadium. Their findings indicate that the hydride phase, either precipitated upon cooling or stress induced, was not solely responsible for the loss in ductility and that hydrogen in solid solution must somehow reduce the surface energy and thereby the associated binding energy or cohesion of vanadium.

Hydrogen embrittlement of the hexagonal close packed metals zirconium and titanium has been investigated by several authors (22,24,25,

31,32). The majority of the evidence suggests that the fracture properties are determined primarily by the behavior of precipitated hydrides. Westlake's study on Zr (24) revealed that embrittlement as measured by loss in reduction of area can be attributed to cracking of precipitated hydrides in a ductile matrix. However, it should be noted that the critical step in the fracture process was not the nucleation of cracks, but the propagation of nucleated cracks in a "ductile" matrix. Similar behavior has been observed in titanium. Furthermore, Beevers and Edmonds (32) have shown that increasing the oxygen content in Ti resulted in enhanced embrittlement at a given hydrogen content. Thus, it has not been possible to determine whether hydrogen in solid solution can in fact embrittle HCP metals because of the very low solid solubilities of hydrogen at low temperatures and because of the effect of interstitial or substitutional impurities on the mechanical properties of hydrogenated Zr or Ti.

In contrast, this investigation revealed that scandium can be embrittled by the addition of 14.14 at% H at room temperature (295 K), and that the ductility as measured by percent uniform elongation and reduction of area is a strong function of hydrogen content and temperature. Additions of up to 8.80 at% H had small effects on the ductility parameters when compared to unhydrogenated scandium. Examination of the surfaces of the 8.80 at% hydrogen alloy revealed that the fracture at all temperatures was by shear and that no cracks were formed during deformation. However, with the addition of 14.14 at% H, embrittlement was observed as revealed by the fracture surface and the onset of a

ductile-to-brittle transition. Increasing the hydrogen content even further as well as the strain rate caused the ductile-to-brittle transition to shift to higher temperatures as shown in Figs. 12 and 15. The fracture surfaces of samples that failed in the brittle region revealed that the macroscopic fracture mode was cleavage. Optical microscopy of sectioned specimens showed transgranular fracture and a number of transgranular secondary cracks, the density of which increased as the fracture surface was approached. Cracks did not appear to nucleate preferentially at grain boundaries or twins.

From the phase diagram shown in Fig. 1 the hydrogen solid solubility limit of scandium at room temperature is approximately 33 at%. Even though this value was extrapolated from high temperature pressure-composition data (34,35), it is in good agreement with room temperature X-Ray studies done by Azarkh and Funin (33), who reported that 30 at% H is the solubility limit at room temperature. Furthermore, a number of techniques are available to determine the solvus curve at subambient temperatures such as resistivity measurements and optical metallography to name a few. Westlake (37) used resistivity measurements to determine the vanadium-rich end of the V-H system whereas Sherman et al. (30) used metallographic techniques. The results were in excellent agreement. In a recent study of the zirconium-hydrogen system, Cann and Atrens (38) used metallographic techniques to determine the solvus curve at low temperatures. Jensen and Zalesky (36) in a resistivity study of the scandium-hydrogen alloys employed in the present investigation have shown that hydrides were not

formed upon cooling to 4.2 K. Additional evidence for the absence of a hydride precipitation was found from metallographic examination at subambient temperatures of the hydrogen charged specimens. It is also believed that hydrides could not have been stress induced in scandium, because Beardsley's study (39) on vanadium hydrides revealed that the hydride phase cannot be stress induced to precipitate above its stress-free precipitation temperature, i.e. above the solvus curve. Therefore, it must be concluded that hydrogen embrittlement of scandium was in fact caused by hydrogen dissolved in solid solution.

The addition of hydrogen produced a number of interesting features, in some cases unexpected, on the strength and flow stress behavior of scandium. With the initial addition of 2.12 at% H, solution softening was observed at all test temperatures. "Solution softening" implies that the strength is decreased by alloying with either interstitial or substitutional elements. There are three solution softening theories; (1) a localized reduction of the Peierls-Naborro stress, (2) changes in the mobile dislocation density, and (3) a scavenging mechanism. Studies by Gibala and co-workers (40,41,42) on body centered cubic metals revealed that the scavenging mechanism is consistent with their results. The scavenging mechanism is explained in terms of the association between substitutional and interstitial solutes and between interstitials of the same or different types in solid solution to form clusters. The formation of clusters could reduce the total number of obstacles to dislocation motion.

The onset of an upper and lower yield point was observed with the addition of 8.80 at% H at 78 K, indicating that hydrogen could be pinning dislocations. From the temperature-concentration curve shown in Fig. 6 it can be seen that as the hydrogen content in scandium is increased the temperature range over which yield points are induced increases.

One of the more interesting results of this investigation was found when log flow stress was plotted versus temperature for various scandium-hydrogen alloys. It was observed that the data were divided into three regions as shown in Figs. 23 through 27. However, the temperature dependence of the flow stress does not correlate with the embrittlement of scandium at concentrations higher than 8.80 at% H. For example, although the rapid increase in flow stress of the 14.14 at% H material below 295 K tends to correlate with the ductile-to-brittle transition temperature range, the 20.83 at% H material has a ductile-to-brittle transition temperature above 400 K but the flow stress rise occurs below 295 K. Consequently, the appearance of three regions in the log flow stress-temperature behavior does not explain embrittlement but is apparently a reflection of the effect of hydrogen on the deformation modes or strengthening.

From Fig. 30 where the yield strength is plotted as a function of concentration for all temperatures employed, it can be seen that the degree of strengthening due to hydrogen in solid solution is temperature dependent. When one compares the strengthening of scandium containing 0.20 at% H to scandium containing 14.14 at% H as a function of decreasing temperature, there is a pronounced difference at temperatures

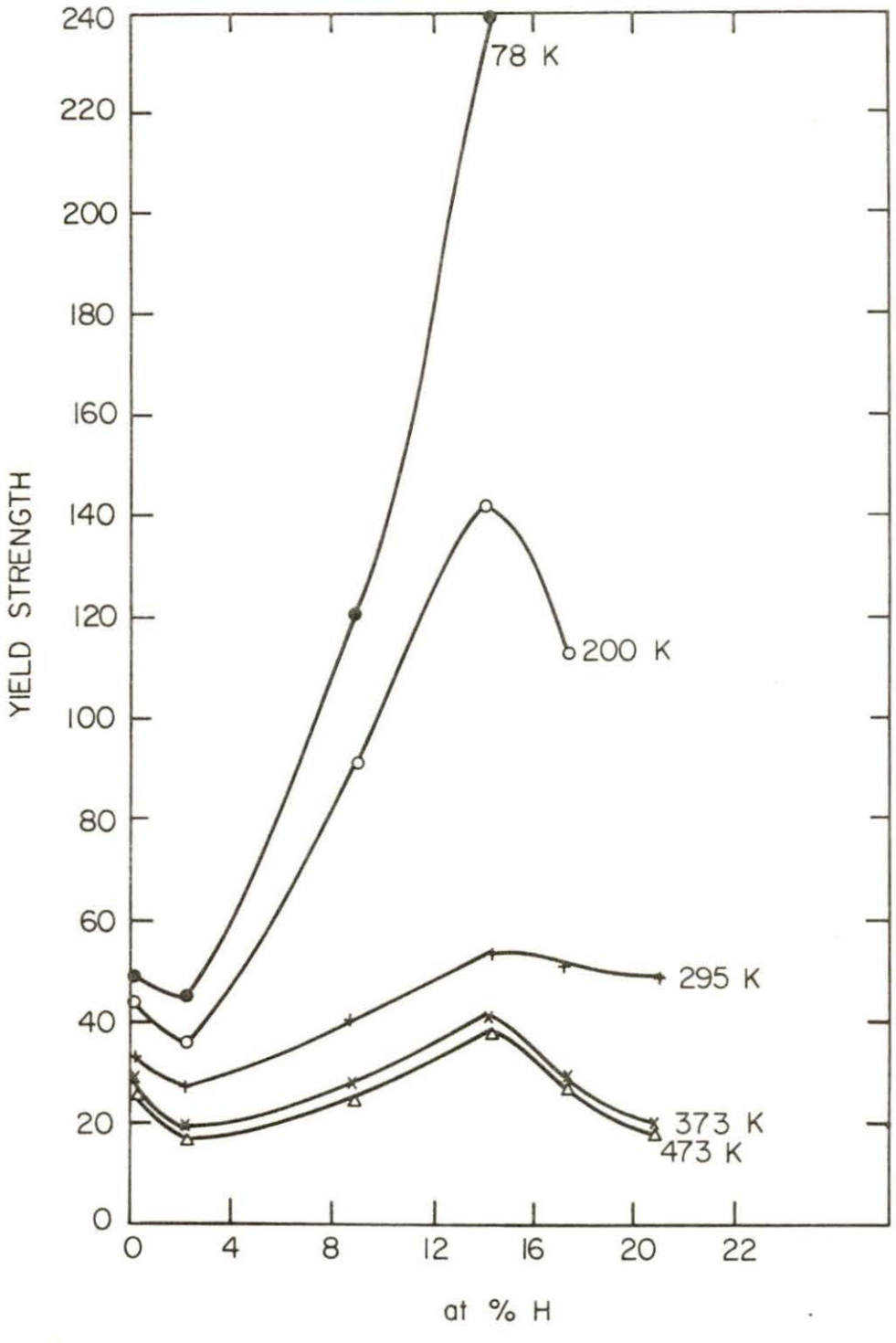

Fig. 30. Yield strength versus hydrogen concentration at given temperatures

below 295 K. Furthermore, there appears to be three regions of strengthening namely, (1) potent strengthening at temperatures of 200 K and below, (2) gradual strengthening in the temperature range of 373 K and 200 K, and (3) small amount of strengthening at temperatures of 373 K and higher. Therefore, it appears that the onset of the three regions when log flow stress versus temperature is plotted is a direct result of low temperature strengthening.

The two most commonly used strengthening models are, (1) that of Fleischer (43) who predicted that the stress should be proportional to the square root of the solute concentration and (2) that of Labusch (44) who predicted that the stress should be proportional to the two-thirds power of the solute concentration. Attempts were made to fit the limited number of data points available to these models. The results indicate that, at temperatures below 295 K neither model fits the data. On the other hand, at temperatures of 295 K and higher the data plotted equally linearly versus concentration to the one-half or two-thirds power. Therefore no conclusion can be reached about a particular strengthening model at this point. Comparison of the results obtained in this study with other hexagonal close packed metals, such as Zr and Ti, have not been made because strengthening in these metals is complicated by the fact that hydrogen precipitates at subambient temperatures as hydrides. Hence, the tensile properties of Zr and Ti hydrogen alloys are due to a combination of precipitation hardening and solution strengthening rather than simple solution hardening.

The pseudo-activation volume for scandium containing 14.14 at% H

as calculated from strain rate changes at a given temperature is plotted versus stress in Fig. 31. The pseudo-activation volume data for "pure" scandium (0.20 at% H) is also included in Fig. 31. The two curves are very similar and at high stresses (low temperatures) the "pure" scandium pseudo-activation volumes tend to approach the 14.14 at% H curve. The pseudo-activation volumes for 14.14 at% H were nearly independent of stress at higher stresses but increased rapidly with stress at low stresses. The nearly stress independent portion of the 14.14 at% H curve indicates that at low temperatures there is not sufficient thermal energy for dislocations to overcome hydrogen atoms. At higher temperatures the dislocations may still be pinned, however there is enough thermal energy to overcome pinning resulting in a stress-dependent pseudo-activation curve. This result coupled with the fact that hydrogen caused considerable strengthening and induced concentration-dependent yield points permits the conclusion that; hardening is attributable to the interaction between hydrogen atoms and dislocations.

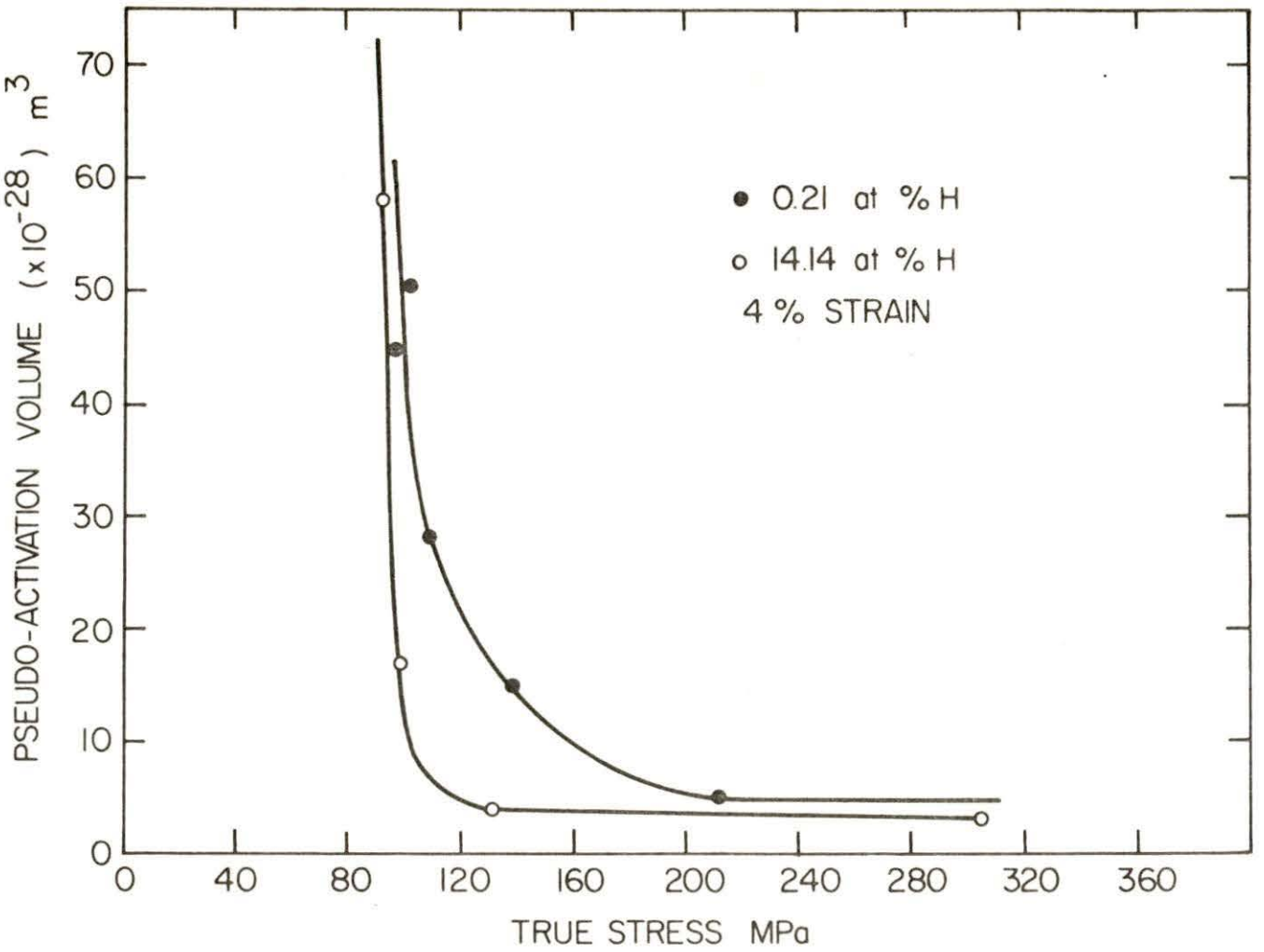

Fig. 31. Pseudo-activation volume versus true stress for scandium containing 0.20 and 14.14 at% H

SUMMARY AND CONCLUSION

The main reason for conducting this investigation was to determine whether scandium, a hydride forming metal, can be embrittled by hydrogen disolved in solid solution. It was demonstrated that embrittlement or severe loss in ductility was observed with the addition of 14.14 at% H at 78 K and that at room temperature (295 K) embrittlement occurred with the addition of 20.83 at% H. Subambient resistivity measurements and metallographic results revealed no evidence of precipitated scandium hydrides in the range of test temperatures used in this investigation. Therefore the embrittlement of hydrogen charged scandium is due to hydrogen in solid solution.

In addition it was found that hydrogen strengthened scandium substantially at low temperatures and produced discontinuous yielding over a temperature range which was concentration dependent. The yield strength data in the concentration range of 2.12 to 14.14 at% H and at temperatures greater than 295 K plotted equally well to hardening models proposed by Labusch and Fleischer, whereas at temperatures below 295 K the data did not follow either model.

REFERENCES CITED

1. C. T. Horovitz, K. A. Gschneidner Jr., G. A. Melson, D. H. Youngblood and H. H. Schock, "Scandium, Its Occurrence, Chemistry, Physics, Metallurgy, Biology and Technology," Academic Press, New York, 1975, p. 39

2. F. H. Spedding and A. H. Daane, "The Rare Earths," Wiley, New York, 1961 p. 428.

3. J. O. Betterton and J. O. Scarbrough, Phys. Rev., 168, 715 (1968).

4. D. Geiselman, J. Less Common Metals, 4, 362 (1962).

5. L. D. Sokolov, V. M. Skudnov, A. M. Shneyberg and A. N. Gladkikh, Tzv. Akad. Nauk. SSSR, Metally, 2 Eng. transl., Russ. Met., 2, 106 (1970).

6. F. H. Spedding and J. J. Croat, J. Chem. Phys., 58, 5514 (1973).

7. J. E. Hilliard, Met. Prog., 87, 150 (1964).

8. B. G. Koepke, E. D. Gibson and T. E. Scott, Trans. ASM, 60, 409 (1967).

9. C. V. Owen and T. E. Scott, J. Less Common Metals, 16, 447 (1968).

10. C. V. Owen and T. E. Scott, J. Less Common Metals, 37, 113 (1974).

11. C. V. Owen and T. E. Scott, J. Less Common Metals, 30, 353 (1973).

12. C. V. Owen and T. E. Scott, J. Less Common Metals, 25, 161 (1971).

13. K. A. Gschneidner Jr., L. Eyring, "Handbook on the Physics and Chemistry of Rare Earths," North-Holland, Amsterdam, 1979, p.

14. H. Conrad, J. Metals, 100, 582 (1964).

15. H. Conrad in "High Strength Materials," V. F. Zackay, Ed.; Wiley, New York, 1965, p. 436.

16. D. H. Baldwin and R. E. Reed-Hill, Trans AIME, 242, 661 (1968).

17. D. H. Sastry, Y.V.R.K. Prasad and K. I. Vasec, J. Mater. Sci., 6, 332 (1971).

18. H. Conrad, Acta Met., 14, 1631 (1966).

19. K. Okazaki and H. Conrad, Acta Met., 21, 1117 (1973).

20. D. G. Westlake, J. Nuc. Mat., 16, 215 (1965).

21. T. W. Wood and R. D. Daniels, Trans. AIME, 233, 898 (1965).

22. C. J. Beevers, Trans. AIME, 233, 780 (1965).

23. W. H. Erickson and D. Hardie, J. Nuc. Mat., 45, 265 (1973).

24. D. G. Westlake, Trans. ASM, 56, 1 (1963).

25. R. P. Marshall, J. Nuc. Mat., 24, 34 (1967).

26. M. R. Louthan, Jr., Trans. AIME, 227, 1116 (1963).

27. G. J. Simpson and C. E. Ells, J. Nuc. Mat., 52, 289 (1974).

28. M. Cornet and S. Talbot-Besnard in "Mechanisms of Environment Sensitive Cracking," P. R. Swann, F. P. Ford, and A.R.C. Westwood, Eds., The Metals Society, London, 1978, p. 538.

29. T. Boniszewski and G. C. Smith, Acta Met., 11, 165 (1963).

30. D. H. Sherman, C. V. Owen, and T. E. Scott, Trans. AIME, 242, 1775 (1968).

31. N. E. Paton and J. C. Williams in "Hydrogen in Metals," I. M. Bernstein and A. W. Thompson, Eds., ASM, Metals Park, Ohio, 1967, p. 409.

32. C. J. Beevers and D. V. Edmonds, Trans. AIME, 245, 2391 (1969).

33. Z. M. Azarkh and V. N. Funin, Soviet Phys.-Crystallography, 10, 21 (1965).

34. J. F. Stampfer, U.S. Atomic Energy Comm. Rept. LA-3473 (1966).

35. M. L. Lieberman and P. G. Wahlbeck, J. Phys. Chem., 69, 3514 (1965).

36. C. L. Jensen and M. P. Zalesky, J. Less Common Metals, accepted for publication.

37. D. G. Westlake, Trans. AIME, 239, 1341 (1967).

38. C. D. Cann and A. Atrens, J. Nuc. Mat., 88, 42 (1980).

39. M. B. Beardsley, M.S. Thesis, Iowa State University, Ames, Iowa, 1977.

40. K. V. Ravi and R. Gibala, Scripta Met., 3, 547 (1969).

41. A. A. Sagues, M. G. Ulitchny, and R. Gibala in "Effect of Hydrogen on Behavior of Materials," A. W. Thompson and I. M. Bernstein, Eds., AIME, New York, 1976, p. 393.

42. M. G. Ulitchny and R. Gibala in "L'Hydrogene dans les Metaux," P. Bastien, Ed., Editions Science et Industrie, Paris, 1972, p. 128.

43. R. L. Fleischer, J. App. Phys., 33, 3504 (1962).

44. R. Labusch, Phys. Stat. Solidi, 41, 659 (1970).

ACKNOWLEDGEMENTS

This work was accomplished with the help, cooperation and encouragement from many people. I appreciate the help and guidance I received from Professor J. D. Verhoeven and Mr. D. E. Williams during my stay at Iowa State University. I also wish to express my appreciation to Professor D. T. Peterson and Dr. C. L. Jensen for their interest in this work and the resistivity studies. I particullarly want to thank my Advisor and Major Professor T. E. Scott for his helpful advice, continued interest during this investigation, and critical analysis in the preparation and completion of this work. The experimental assistance of C. W. Owen, L. K. Reed, and A. D. Johnson in sample preparation as well as the helpful guidance of H. H. Baker in the metallography lab is gratefully acknowledged. Many thanks are due to Metallurgy Group XIII in general as well as the coffee friends for making my stay a pleasant experience. I also have to thank my mother and my wife, Judy, who have given me the support and occasional shove I needed to complete the thesis when it did not seem worth the effort.

Finally, I would like to thank this country and Iowa State University for providing an education and above all a chance to grow up and learn the meaning of freedom without political pressures.